INSTITUT FÜR INFORMATIK

A Novel Representation for Two-dimensional Image Structures

Di Zang and Gerald Sommer

Bericht Nr. 0606
June 2006

CHRISTIAN-ALBRECHTS-UNIVERSITÄT

KIEL

Institut für Informatik
der Christian-Albrechts-Universität zu Kiel
Olshausenstr. 40
D – 24098 Kiel

A Novel Representation for Two-dimensional Image Structures

Di Zang and Gerald Sommer

e-mail: {zd,gs}@ks.informatik.uni-kiel.de

Dieser Bericht ist als persönliche Mitteilung aufzufassen.

ABSTRACT

This paper presents a novel approach towards two-dimensional (2D) image structures modeling. To obtain more degrees of freedom, a 2D image signal is embedded into a certain geometric algebra. Coupling methods of differential geometry, tensor algebra, monogenic signal and quadrature filter, we can design a general model for 2D structures as the monogenic extension of a curvature tensor. Based on it, a local representation for the intrinsically two-dimensional (i2D) structure is derived as the monogenic curvature signal. From it, independent features of local amplitude, phase and orientation are simultaneously extracted. Besides, a monogenic curvature scale-space can be built by applying a Poisson kernel to the monogenic curvature signal. Compared with the other related work, the remarkable advantage of our approach lies in the rotationally invariant phase evaluation of 2D structures in a multi-scale framework, which delivers access to phase-based processing in many computer vision tasks.

CONTENTS

1. INTRODUCTION

Model based image representation plays an important role in many computer vision tasks such as object recognition, motion estimation, image retrieval, etc. Therefore, signal modeling for local structures is of high significance in image processing. There are bulk of researches for intensity-based modeling, see [18, 27, 29, 12, 13]. However, those approaches are not stable when the illumination varies. Therefore, that intensively investigated area of research is not adequate to model local structures. On the other hand, phase information carries most essential structure information of the original signal [34]. It is invariant with respect to illumination changes. Consequently, modeling of local structures should take both the intensity and phase information into consideration.

In one dimensional (1D) signal processing, the analytic signal [20] is an important complex valued model which can be used for speech recognition, seismic data analysis, airfoil design and so on. The polar representation of the analytic signal yields the local amplitude and local phase, which are measures of quantitative and qualitative information of a signal, respectively. In 1D case, there exist four types of structures, they are the peak, pit, decreasing slope and increasing slope. The local amplitude is invariant with respect to local structures and it indicates the energetic information of the signal. The local phase allows to distinguish structures and it is invariant with respect to the local amplitude. If the local structure varies, the local phase will correspondingly change. Local amplitude and local phase are independent of each other and they fulfill the properties of invariance and equivariance. Invariance means that a feature value is not changed by a certain group acting on a signal. Opposite to invariance, equivariance means there is a monotonic dependency of a feature value on the parameter of the group action. If a set of features includes only invariant and equivariant features, it thus has the property of invariance-equivariance. In addition to satisfying the requirement of invariance and equivariance, if a set of features is at the same time a unique description of the signal, it then performs a split of identity [21]. The split of identity indicates that different features represent mutually different properties of the signal and the whole set of features describes completely the signal. Hence, the analytic signal performs a split of identity.

In 2D images, there exist infinite many types of structures. These can be classified with different features such as their intrinsic dimensions, the number and shape of junctions, or the type of curvature in a differential geometric setting. According to their intrinsic dimensionality, 2D images can locally belong to the intrinsically zero dimensional (i0D) signals which are constant signals, intrinsically one dimensional (i1D) signals representing straight lines and edges and intrinsically two dimensional (i2D) signals which do not belong to the above two cases. The i2D structures are composed of curved edges and lines, junctions, corners and line ends, etc. Intrinsic dimensionality

[40] is a local property of a multidimensional signal, which expresses the number of degrees of freedom necessary to describe local structure. The term intrinsic dimension used in image processing corresponds to the term codimension in mathematics. In [40], a discrete concept of the intrinsic dimensionality has been proposed and it was later extended to a continuous one by Krüger and Felsberg [30]. The i1D and i2D structures carry most of the important information of the image, therefore, correct characterization of them has great significance for many computer vision applications.

Many approaches have been proposed for the signal representation of local image structures. The structure tensor [18] and the boundary tensor [27] estimate the main orientation and the energy of the i2D signal. However, the split of identity is lost, because the phase is neglected. In [29], a nonlinear image operator for the detection of locally i2D signals was proposed, but it captures no information about the phase. There are lots of papers concerned with applications of the analytic signal for image analysis. But they have serious problems in transferring that concept from 1D to 2D in a rotation-invariant way. The partial Hilbert transform and the total Hilbert transform [22] provide some representations of the phase in 2D. Unfortunately, they lack the property of rotation invariance and are not adequate for detecting i2D features. Bülow and Sommer [6] proposed the quaternionic analytic signal, which enables the evaluation of the i2D signal phase, however, this approach also has the drawback of being not rotationally invariant. For i1D signals, Felsberg and Sommer [14] proposed the monogenic signal as a novel model. It is a rotationally invariant generalization of the analytic signal in 2D and higher dimensions. In [28], the 3D monogenic signal has been used for image sequence analysis. From the monogenic signal, the local amplitude and a local phase representation can be simultaneously extracted. They deliver an orthogonal decomposition of the original signal into amplitude, phase and orientation. Thus, the monogenic signal has the property of split of identity [14]. However, it captures no information of the i2D part. A 2D phase model is proposed in [10], where the i2D signal is split into two perpendicularly superposed i1D signals and the corresponding two phases are evaluated. The operator derived from that signal model takes advantage of spherical harmonics up to order three. It delivers a new description of i2D structure by a so-called structure multivector. Unfortunately, steering is needed and only i2D patterns superimposed by two perpendicular i1D signals can be correctly handled. Quite another approach of local signal analysis is based on differential geometry of curves and surfaces [25, 26]. The main points of concern are some invariance properties of signal analysis and regional symmetry with respect to certain combinations of Gaussian and mean curvatures of local surface patterns in a Gaussian multi-scale framework [17, 16]. We will pick up the differential geometry model of surfaces. But instead of a Gaussian blurring operator, we will apply a Poisson blurring operator as a consequence of the algebraic embedding we use.

Our purpose is to build a general model for all 2D structures without necessarily delivering all parameters for describing the local structure. This model should contain both the amplitude and phase information of 2D structures in a rotation-invariant manner. In other words, the new model should be an extension of the analytic signal to the 2D case. In this paper, we present a novel signal model which covers 2D structures of all intrinsic dimensionalities. By embedding our problem into a certain geometric

algebra, more degrees of freedom can be obtained to derive a complete representation for the 2D structure. Based on the differential geometry, we are able to design that general model for 2D structures in a rotation-invariant manner by coupling the methods of tensor algebra, monogenic signal and quadrature filter. The proposed model can be considered as the monogenic extension of a curvature tensor. From this model, a local signal representation for i1D structures is obtained. It is exactly the monogenic signal [14] as a special case of this general model. The local representation for i2D structures, referred as the monogenic curvature signal, can also be derived based on the proposed model.

From the monogenic curvature signal, three independent local features can be extracted. They are the amplitude, phase and orientation just like in the case of the monogenic signal. Hence, the monogenic curvature signal also performs the split of identity, i.e., the invariance-equivariance property of signal decomposition. The energy output (square of the amplitude) can be regarded as a junction strength for detecting the points of interest. The estimated orientation represents the local main orientation of the structure and the phase feature can be used to classify some specific i2D structures.

The amplitude, orientation and phase are coupled to a scale concept in one single framework which is called the monogenic curvature scale-space. The monogenic curvature scale-space is the scale-space of the monogenic curvature signal. But instead of considering that unifying framework, the orthogonal scale-spaces for amplitude, phase and orientation can also be studied separately for local signal analysis. These features are scale dependent, but they are still independent of each other at each scale space. The monogenic curvature scale-space is completely different to the well-known Gaussian curvature scale-space [33, 32]. Both the definition of curvature and the scale generating operator are different. Compared with the related research work, our main contribution is the derivation of a general signal model for 2D structures, which enables us to simultaneously extract local features in a multi-scale way. The remarkable advantage lies in the possibility of evaluating the 2D structure phase information in a rotation-invariant manner, which gives access to many phase-based processing in computer vision tasks.

The rest of this paper is organized as follows. Section 2 introduces the mathematical preliminaries, which includes geometric algebra, basis functions and the monogenic scale-space. In Section 3, a brief introduction to the differential geometry is given and the general signal model for 2D image structures is presented. Section 4 gives a detailed interpretation of the monogenic curvature signal. Parity symmetry analysis of the monogenic curvature signal is given in Section 5. In Section 6, we introduce the monogenic curvature scale-space. Finally, we conclude this paper in Section 7.

2. MATHEMATICAL PRELIMINARIES

The way we intend to design a general model for 2D structures is a generalization of the analytic signal. It cannot be realized in the domain of complex numbers. Instead, a more powerful algebraic system should be taken into consideration. Geometric algebras constitute a rich family of algebras as generalization of vector algebra [24]. Compared with the classical framework of vector algebra, the geometric algebra makes available a tremendous extension of modeling capabilities. By embedding our problem into a certain geometric algebra, more degrees of freedom can be obtained, which makes it possible to extract multiple features of 2D structure. For the problem we are concerned, the 2D signal will be algebraically embedded into the Euclidean 3D space $\mathbb{R}^3$. Therefore, in this section, we give a brief introduction to the geometric algebra over 3D Euclidean space ($\mathbb{R}_3$). For the detail information, please refer to [31, 1, 23].

2.1 Geometric algebra of 3D Euclidean space $\mathbb{R}^3$

The Euclidean space $\mathbb{R}^3$ is spanned by the orthonormal basis vectors $\{\mathbf{e}_1, \mathbf{e}_2, \mathbf{e}_3\}$. The geometric algebra of the 3D Euclidean space ($\mathbb{R}_3$) consists of $2^3 = 8$ basis elements,

$$\mathbb{R}_3 = span\{1, \mathbf{e}_1, \mathbf{e}_2, \mathbf{e}_3, \mathbf{e}_{23}, \mathbf{e}_{31}, \mathbf{e}_{12}, \mathbf{e}_{123} \equiv I_3\} \tag{2.1}$$

Here $\mathbf{e}_{23}$, $\mathbf{e}_{31}$ and $\mathbf{e}_{12}$ are the unit bivectors and the element $\mathbf{e}_{123}$ is a unit trivector or unit pseudoscalar. A general combination of these elements is called a multivector, e.g. $M = a + b\mathbf{e}_1 + c\mathbf{e}_2 + d\mathbf{e}_3 + e\mathbf{e}_{23} + f\mathbf{e}_{31} + g\mathbf{e}_{12} + hI_3$. The basic product of the geometric algebra is the geometric product. The geometric product of two multivectors M_1 and M_2 is indicated by juxtaposition of M_1 and M_2, i.e. M_1M_2. The multiplication results of the basis elements are shown in table 1. The geometric product of two vectors $\mathbf{x} = x_1\mathbf{e}_1 + x_2\mathbf{e}_2$ and $\mathbf{y} = y_1\mathbf{e}_1 + y_2\mathbf{e}_2$ can be decomposed into their inner product ($\cdot$) and outer product ($\wedge$),

$$\mathbf{x}\mathbf{y} = \mathbf{x} \cdot \mathbf{y} + \mathbf{x} \wedge \mathbf{y} \tag{2.2}$$

where the inner product of $\mathbf{x}$ and $\mathbf{y}$ is $\mathbf{x} \cdot \mathbf{y} = x_1y_1 + x_2y_2$ and the outer product is $\mathbf{x} \wedge \mathbf{y} = (x_1y_2 - x_2y_1)\mathbf{e}_{12}$.

Due to the orthogonality of basis vectors, their outer product is equivalent to their geometric product.

$$\mathbf{e}_1 \wedge \mathbf{e}_2 = \mathbf{e}_1\mathbf{e}_2 \equiv \mathbf{e}_{12} \tag{2.3}$$

$$\mathbf{e}_2 \wedge \mathbf{e}_3 = \mathbf{e}_2\mathbf{e}_3 \equiv \mathbf{e}_{23} \tag{2.4}$$

$$\mathbf{e}_3 \wedge \mathbf{e}_1 = \mathbf{e}_3\mathbf{e}_1 \equiv \mathbf{e}_{31} \tag{2.5}$$

The k-grade part of a multivector is obtained from the grade operator $\langle M \rangle_k$. A blade of grade k, i.e. a k-blade B_k, is the outer product ($\wedge$) of k independent vectors $\mathbf{x}_1, ..., \mathbf{x}_k \in \mathbb{R}^3$,

$$B_k = \mathbf{x}_1 \wedge ... \wedge \mathbf{x}_k = \langle \mathbf{x}_1 ... \mathbf{x}_k \rangle_k \tag{2.6}$$

Hence, $\langle M \rangle_0$ is the scalar part of M, $\langle M \rangle_1$ represents the vector part, $\langle M \rangle_2$ indicates the bivector part and $\langle M \rangle_3$ is the trivector part, which commutes with every element of $\mathbb{R}_3$. The dual of a multivector M is defined to be the product of M with the inverse of the unit pseudoscalar I_3

$$M^* = M I_3^{-1} = -M I_3 \tag{2.7}$$

The modulus of a multivector is obtained by $|M| = \sqrt{\langle M \widetilde{M} \rangle_0}$, where $\widetilde{M}$ is the reverse of a multivector defined as $\widetilde{M} = \langle M \rangle_0 + \langle M \rangle_1 - \langle M \rangle_2 - \langle M \rangle_3$. The main automorphism of $\mathbb{R}_3$ is the grade involution

$$\widehat{M} = \langle M \rangle_0 - \langle M \rangle_1 + \langle M \rangle_2 - \langle M \rangle_3 \tag{2.8}$$

Combining the grade involution and reversion will yield the conjugation

$$\overline{M} = \widehat{\widetilde{M}} = \langle M \rangle_0 - \langle M \rangle_1 - \langle M \rangle_2 + \langle M \rangle_3 \tag{2.9}$$

A versor is any multivector that can be expressed as the geometric product of invertible vectors, for example,

$$U = \mathbf{x}_k ... \mathbf{x}_2 \mathbf{x}_1 \tag{2.10}$$

where the choice of vectors is not unique, but there is a minimal number $k \leq n$ with n denoting the dimension of the vector space. The parity of U is even (odd) for even (odd) k. An even versor R is called a spinor if

$$R \widetilde{R} = |R|^2 \tag{2.11}$$

where $\widetilde{R}$ indicates the reversion of the even versor R. In the case of $|R|^2 = 1$, the spinor is called a rotor.

In $\mathbb{R}_3$, an even grade multivector is called a spinor,

$$S = a + e\mathbf{e}_{23} + f\mathbf{e}_{31} + g\mathbf{e}_{12} \quad \text{with} \quad S\widetilde{S} = |S|^2 \tag{2.12}$$

All spinors form a proper subalgebra of $\mathbb{R}_3$, that is the even subalgebra $\mathbb{R}_3^+$. A spinor represents a scaling-rotation, i.e. $S = r\exp(\theta B)$, where B is a bivector indicating the rotation plane, θ is the rotation angle within that plane and r refers to the scaling factor. There exist isomorphisms between the algebra of complex numbers and the subalgebras of $\mathbb{R}_3$, which are generated by $\{1, I_3\}$ or $\{1, \frac{B}{|B|}\}$ with $\frac{B}{|B|}$ being a normalized bivector. It is shown in table 1 that the square of the bivectors or trivector equals -1, therefore, the imaginary unit i of the complex numbers can be substituted by a bivector or a trivector, yielding an algebra isomorphism.

Tab. 2.1: The geometric product of basis elements of $\mathbb{R}_3$

	1	$\mathbf{e}_1$	$\mathbf{e}_2$	$\mathbf{e}_3$	$\mathbf{e}_{23}$	$\mathbf{e}_{31}$	$\mathbf{e}_{12}$	I_3
1	1	$\mathbf{e}_1$	$\mathbf{e}_2$	$\mathbf{e}_3$	$\mathbf{e}_{23}$	$\mathbf{e}_{31}$	$\mathbf{e}_{12}$	I_3
$\mathbf{e}_1$	$\mathbf{e}_1$	1	$\mathbf{e}_{12}$	$-\mathbf{e}_{31}$	I_3	$-\mathbf{e}_3$	$\mathbf{e}_2$	$\mathbf{e}_{23}$
$\mathbf{e}_2$	$\mathbf{e}_2$	$-\mathbf{e}_{12}$	1	$\mathbf{e}_{23}$	$\mathbf{e}_3$	I_3	$-\mathbf{e}_1$	$\mathbf{e}_{31}$
$\mathbf{e}_3$	$\mathbf{e}_3$	$\mathbf{e}_{31}$	$-\mathbf{e}_{23}$	1	$-\mathbf{e}_2$	$\mathbf{e}_1$	I_3	$\mathbf{e}_{12}$
$\mathbf{e}_{23}$	$\mathbf{e}_{23}$	I_3	$-\mathbf{e}_3$	$\mathbf{e}_2$	-1	$-\mathbf{e}_{12}$	$\mathbf{e}_{31}$	$-\mathbf{e}_1$
$\mathbf{e}_{31}$	$\mathbf{e}_{31}$	$\mathbf{e}_3$	I_3	$-\mathbf{e}_1$	$\mathbf{e}_{12}$	-1	$-\mathbf{e}_{23}$	$-\mathbf{e}_2$
$\mathbf{e}_{12}$	$\mathbf{e}_{12}$	$-\mathbf{e}_2$	$\mathbf{e}_1$	I_3	$-\mathbf{e}_{31}$	$\mathbf{e}_{23}$	-1	$-\mathbf{e}_3$
I_3	I_3	$\mathbf{e}_{23}$	$\mathbf{e}_{31}$	$\mathbf{e}_{12}$	$-\mathbf{e}_1$	$-\mathbf{e}_2$	$-\mathbf{e}_3$	-1

2.2 Geometric embedding of the signal

The scalar-valued real 2D image signal $f(x, y)$ will be embedded into $\mathbb{R}_3$ as a real-valued vector field, i.e. $f(x, y)\mathbf{e}_3 \equiv \mathbf{f}(\mathbf{x}) = \mathbf{f}(x\mathbf{e}_1 + y\mathbf{e}_2 + z\mathbf{e}_3)$, $\mathbf{x} \in \mathbb{R}^3$ and $z = 0$. Thus, rotating the signal $\mathbf{f}$ out of the $\mathbf{e}_3$ axis results in a representation $\mathbf{f}_M$ which contains additional non-real components. Hence, $\mathbf{f}_M$ takes the following form

$$\mathbf{f}_M(\mathbf{x}) = f_1(\mathbf{x})\mathbf{e}_1 + f_2(\mathbf{x})\mathbf{e}_2 + f_3(\mathbf{x})\mathbf{e}_3 \qquad (2.13)$$

This representation of a 2D signal is called a monogenic signal [14], as the rotationally invariant generalization of the analytic signal. The vector-valued signal $\mathbf{f}_M$ in $\mathbb{R}_3$ can be considered as the impulse response of a spinor S acting on the $\mathbf{e}_3$ basis vector, i.e. $\mathbf{f}_M = \mathbf{e}_3 S$. The transformation performed under the action of the spinor delivers access to both the amplitude and phase information of the vector-valued signal $\mathbf{f}_M$ [39]. To make this clear, we will consider the spinor more in depth. The spinor can be represented in polar coordinates as an exponential form. Therefore, from the logarithm of the spinor, two parts can be obtained. They are the scaling which corresponds to the local amplitude and the rotation which corresponds to the local phase representation. The $\mathbb{R}_3$-logarithm of a spinor $S \in \mathbb{R}_3^+$ takes the following form

$$\log(S) = \langle \log(S) \rangle_0 + \langle \log(S) \rangle_2 = \log(|S|) + \frac{\langle S \rangle_2}{|\langle S \rangle_2|}\text{atan}\left(\frac{|\langle S \rangle_2|}{\langle S \rangle_0}\right) \qquad (2.14)$$

where atan is the arc tangent mapping for the interval $[0, \pi)$. The scalar part $\langle \log(S) \rangle_0 = \log(|S|)$ illustrates the attenuation [15] as the logarithm of the local amplitude. Hence, the local amplitude is obtained as the exponential of it

$$|S| = \exp(\log|S|) = \exp(\langle \log(S) \rangle_0) \qquad (2.15)$$

The bivector part of $\log(S)$ indicates the local phase representation

$$\arg(S) = \langle \log(S) \rangle_2 = \frac{\langle S \rangle_2}{|\langle S \rangle_2|}\text{atan}\left(\frac{|\langle S \rangle_2|}{\langle S \rangle_0}\right) \qquad (2.16)$$

The algebraically embedded Fourier transform of a 2D signal $\mathbf{f}(\mathbf{x})$, see [10], is defined as

$$\mathbf{G}(\mathbf{u}) = \int_{y=-\infty}^{\infty} \int_{x=-\infty}^{\infty} \mathbf{f}(\mathbf{x})\exp(-I_3 2\pi\mathbf{x} \cdot \mathbf{u})dxdy \qquad (2.17)$$

Its corresponding inverse Fourier transform takes the following form

$$\mathbf{f}(\mathbf{x}) = \int_{v=-\infty}^{\infty} \int_{u=-\infty}^{\infty} \mathbf{G}(\mathbf{u}) \exp(I_3 2\pi \mathbf{x} \cdot \mathbf{u}) du dv \qquad (2.18)$$

Hence, given a signal $\mathbf{f}(\mathbf{x}) = f_1(\mathbf{x})\mathbf{e}_1 + f_2(\mathbf{x})\mathbf{e}_2 + f_3(\mathbf{x})\mathbf{e}_3$, its Fourier domain representation reads

$$\mathbf{F}(\mathbf{u}) = \mathcal{F}\{f_1(\mathbf{x})\mathbf{e}_1 + f_2(\mathbf{x})\mathbf{e}_2 + f_3(\mathbf{x})\mathbf{e}_3\} = F_1(\mathbf{u})\mathbf{e}_1 + F_2(\mathbf{u})\mathbf{e}_2 + F_3(\mathbf{u})\mathbf{e}_3 \qquad (2.19)$$

where $\mathcal{F}$ indicates the Fourier transform and F_k ($k = 1, 2, 3$) is the Fourier transform of f_k. For a spinor valued function $h = h_0 + h_{23}\mathbf{e}_{23} + h_{31}\mathbf{e}_{31} + h_{12}\mathbf{e}_{12}$, its spectral domain representation is given by

$$\mathbf{H}(\mathbf{u}) = H_0(\mathbf{u}) + H_{23}(\mathbf{u})\mathbf{e}_{23} + H_{31}(\mathbf{u})\mathbf{e}_{31} + H_{12}(\mathbf{u})\mathbf{e}_{12} \qquad (2.20)$$

where $H_0(\mathbf{u}) = \mathcal{F}\{h_0\}$, $H_{23}(\mathbf{u}) = \mathcal{F}\{h_{23}\}$ and so on.

2.3   Basis functions

In order to analyze 2D patterns, we choose 2D spherical harmonics as basis functions according to the proposal in [10]. Actually, spherical harmonic is a general term which denotes the harmonic oscillations on the unit sphere of a multi-dimensional Euclidean space. However, in this paper, only the spherical harmonics of 2D space are employed, they are also called circular harmonics. Due to the theory of Fourier series, one can approximate any plane angular function (in L_2 sense) by using 2D spherical harmonics. Since the angular behavior of a signal can be regarded as band limited, only spherical harmonics of order zero to three are applied, otherwise, aliasing would occur on a discrete grid around a location $\mathbf{x}$. To build the signal model, we are more concerned of the angular portions. Therefore, we use the polar representation of spherical harmonics instead of the Cartesian form applied in [10].

In the frequency domain, a nth order spherical harmonic H_n takes the following form

$$H_n(\rho, \alpha) = H_n(\rho)H_n(\alpha) = \exp(n\alpha\mathbf{e}_{12}) = \cos(n\alpha) + \sin(n\alpha)\mathbf{e}_{12} \qquad (2.21)$$

where ρ and α denote the polar coordinates in the Fourier domain and n refers to the order of the spherical harmonic. It is obvious that the radial part of the spherical harmonic equals one, i.e. $H_n(\rho) = 1$. Every spherical harmonic consists of two orthogonal components and the first order spherical harmonic is basically identical to the Riesz kernel [14] which is well known in Clifford analysis as the multidimensional generalization of the Hilbert kernel. Since H_n is separable into radial variation and angular variation, and its angular variation is harmonic, according to the theorem in [8] (page 262), its angular variation is preserved in the spatial domain while the radial function is the Hankel transform of the radial variation in the frequency domain. Therefore, the spatial domain representation of a nth order spherical harmonic h_n reads

$$h_n(r, \beta) = c(I_3)^n h_n(r)h_n(\beta) = c(I_3)^n h_n(r)[\cos(n\beta) + \sin(n\beta)\mathbf{e}_{12}] \qquad (2.22)$$
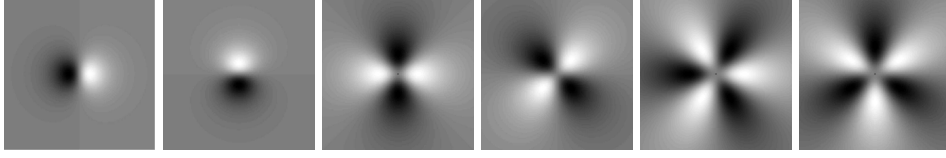
Fig. 2.1: From left to right are spherical harmonic bandpasses of order 1 to 3 in the spatial domain, every spherical harmonic consists of two orthogonal components. White indicates positive one and black represents negative one.

where c indicates a constant, r and β are the polar coordinates in the spatial domain, $h_n(r)$ represents the radial part which is obtained by the nth order Hankel transform of $H_n(\rho)$.

In practice, 2D spherical harmonics are normally considered only as angular parts which should be combined with radial bandpass filters. In this paper, the difference of Poisson (DOP) kernel [10] is employed as the radial bandpass filter, see also the next section. As a result, local signal analysis can be realized in a multi-scale approach in the monogenic scale-space [15]. The DOP is an isotropic bandpass filter which in spectral domain takes the form

$$H_{DOP}(\rho; s) = \exp(-2\pi\rho s_1) - \exp(-2\pi\rho s_2) \tag{2.23}$$

where s_1 and s_2 represent the fine and coarse scales parameters, respectively. Therefore, a nth order bandpass bounded spherical harmonic reads

$$H_n(\rho, \alpha; s) = H_{DOP}(\rho; s)H_n(\alpha) \tag{2.24}$$

Hence, $H_n(\rho, \alpha; s)$ is separable into radial variation $H_{DOP}(\rho; s)$ and angular variation $H_n(\alpha)$. Since the angular portion is harmonic, according to the theorem stated in [8], $H_n(\rho, \alpha; s)$ is separable both in the spatial and spectral domains. Thereby, we are able to obtain the spatial representation of the bandpass bounded spherical harmonic as follows

$$\mathcal{F}^{-1}\{H_n(\rho, \alpha; s)\} = c(I_3)^n h_n(r; s)(\cos(n\beta) + \sin(n\beta)\mathbf{e}_{12}) \tag{2.25}$$

The angular variation is preserved and the radial function $h_n(r; s)$ is the Hankel transform of $H_{DOP}(\rho; s)$. Combined with the DOP bandpass filters, spherical harmonics of order 1 to 3 in the spatial domain are illustrated in Fig. 2.1, where the fine scale is one and the coarse scale takes two.

It is obvious that the amplitude of the spherical harmonic equals always one, that is

$$|H_n^2(\alpha)| = \sqrt{(\cos(n\alpha))^2 + (\sin(n\alpha))^2} = 1 \tag{2.26}$$

If the coordinate system rotates with the angle θ_0, spherical harmonics will rotate accordingly as

$$H_n'(\alpha) = (\cos(n\theta_0)\cos(n\alpha) + \sin(n\theta_0)\sin(n\alpha)) + \tag{2.27}$$
$$(-\sin(n\theta_0)\cos(n\alpha) + \cos(n\theta_0)\sin(n\alpha))\mathbf{e}_{12}$$

The amplitude of the rotated spherical harmonic is

$$
\begin{aligned}
|H_n'^2(\alpha)| = [(\cos(n\theta_0)\cos(n\alpha) + \sin(n\theta_0)\sin(n\alpha))^2 + \\
(-\sin(n\theta_0)\cos(n\alpha) + \cos(n\theta_0)\sin(n\alpha))^2]^{\frac{1}{2}} = 1
\end{aligned}
\tag{2.28}
$$

This results from the fact that no matter what angle the spherical harmonic rotates, its amplitude is always one. Hence, the amplitude of any spherical harmonic is independent of the angular argument. Therefore, using spherical harmonics as basis functions gives access to a rotationally invariant signal representation.

2.4 The monogenic scale-space

In Section 2.2, we have briefly discussed the signal embedding. In that case, a 2D image signal is embedded into 3D Euclidean space as a vector field $\mathbf{f}(\mathbf{x}) = \mathbf{f}(x\mathbf{e}_1 + y\mathbf{e}_2 + z\mathbf{e}_3)$ with $z = 0$. The monogenic signal $\mathbf{f}_M$ [14] is thus obtained by rotating the signal $\mathbf{f}$ out of the $\mathbf{e}_3$ basis vector. This signal representation consists of three components according to Eq. (2.13). There, $f_3(\mathbf{x})\mathbf{e}_3$ indicates the real component which is identical to the original signal $\mathbf{f}(\mathbf{x})$, $f_1(\mathbf{x})\mathbf{e}_1$ and $f_2(\mathbf{x})\mathbf{e}_2$ are two non-real components that can be obtained from the Riesz transform of the original signal.

Let $\mathbf{x} = x\mathbf{e}_1 + y\mathbf{e}_2$ and $\mathbf{u} = u\mathbf{e}_1 + v\mathbf{e}_2$ be the Cartesian coordinates of the spatial domain and the Fourier domain, respectively. The convolution kernel of the Riesz transform is given by

$$
h_R(\mathbf{x}) = -\frac{x}{2\pi|\mathbf{x}|^3}\mathbf{e}_{31} + \frac{y}{2\pi|\mathbf{x}|^3}\mathbf{e}_{23} = \frac{\mathbf{x}\mathbf{e}_3}{2\pi|\mathbf{x}|^3}
\tag{2.29}
$$

and its frequency domain representation reads

$$
H_R(\mathbf{u}) = \frac{\mathbf{u}}{|\mathbf{u}|}I_2^{-1}
\tag{2.30}
$$

In terms of polar coordinates, the spatial and spectral domain representations of the Riesz kernel take the following forms

$$
h_R(r, \beta) = \frac{1}{2\pi r^2}(-\cos(\beta)\mathbf{e}_{31} + \sin(\beta)\mathbf{e}_{23})
\tag{2.31}
$$

$$
H_R(\rho, \alpha) = -\cos(\alpha)\mathbf{e}_2 + \sin(\alpha)\mathbf{e}_1
\tag{2.32}
$$

The Riesz kernel consists of two bivector valued components and it is basically identical to the first order spherical harmonic. Combining the signal and its Riesz transformed result yields the monogenic signal

$$
\mathbf{f}_M(\mathbf{x}) = \mathbf{f}(\mathbf{x}) + (h_R * \mathbf{f})(\mathbf{x})
\tag{2.33}
$$

The real part $\mathbf{f}(\mathbf{x})$ is also called the even component of the monogenic signal. The odd component of the monogenic signal, called the figure flow, is defined as $(h_R * \mathbf{f})(\mathbf{x})$, which is in quadrature phase relation to the even part.

In the light of the discussion in Section 2.2, $\mathbf{f}_M(\mathbf{x})$ can be regarded as the impulse response of a spinor S acting on the $\mathbf{e}_3$ basis vector. Therefore, the logarithm of this spinor gives access to both the amplitude and phase information of the original signal. The spinor field which maps the $\mathbf{e}_3$ basis vector to the vector valued signal $\mathbf{f}_M(\mathbf{x})$ is $\mathbf{e}_3\mathbf{f}_M(\mathbf{x})$. Hence, according to Eq. (2.15) and Eq. (2.16), the local amplitude and local phase representation of the monogenic signal are obtained as follows

$$A_M(\mathbf{x}) = |\mathbf{f}_M(\mathbf{x})| = \exp(\log|\mathbf{e}_3\mathbf{f}_M(\mathbf{x})|) = \exp(\langle\log(\mathbf{e}_3\mathbf{f}_M(\mathbf{x}))\rangle_0) \tag{2.34}$$

$$\Phi_M(\mathbf{x}) = \langle\log(\mathbf{e}_3\mathbf{f}_M(\mathbf{x}))\rangle_2 = \frac{\langle\mathbf{e}_3\mathbf{f}_M(\mathbf{x})\rangle_2}{|\langle\mathbf{e}_3\mathbf{f}_M(\mathbf{x})\rangle_2|}\text{atan}\left(\frac{|\langle\mathbf{e}_3\mathbf{f}_M(\mathbf{x})\rangle_2|}{\langle\mathbf{e}_3\mathbf{f}_M(\mathbf{x})\rangle_0}\right) \tag{2.35}$$

It is also possible to extend the monogenic signal to higher dimensions, see [39, 28]. Hence, the monogenic signal can be regarded as a generalization of the analytic signal in 2D and higher dimensions. The monogenic signal is a novel model for i1D signals, however, it delivers no information about the i2D parts of the 2D image.

Up to now, we only considered the 2D image signal $\mathbf{f}(\mathbf{x}) = \mathbf{f}(x\mathbf{e}_1 + y\mathbf{e}_2 + z\mathbf{e}_3)$ with $z = 0$. If we investigate the case for the half space $z > 0$, this signal will become a smoothed version of the original signal ($z = 0$). Hence, z is regarded as a scale parameter. Applying a Poisson kernel to the original signal results in a smoothed signal which, for all scale parameters s, results in a Poisson scale-space [15],

$$p(\mathbf{x}; s) = (\mathbf{f} * h_P)(\mathbf{x}) \tag{2.36}$$

where s denotes the scale parameter, $p(\mathbf{x}; s)$ is the Poisson scale-space and h_P indicates the scalar valued Poisson kernel defined as

$$h_P(\mathbf{x}) = \frac{s}{2\pi(|\mathbf{x} + s\mathbf{e}_3|)^3} \tag{2.37}$$

and

$$\mathcal{F}\{h_P(\mathbf{x})\} = \exp(-2\pi|\mathbf{u}|s) \tag{2.38}$$

Here $\mathcal{F}$ refers to the Fourier transform. The harmonic conjugate of the Poisson scale-space reads

$$\mathbf{q}(\mathbf{x}; s) = (\mathbf{f} * h_Q)(\mathbf{x}) \tag{2.39}$$

where h_Q denotes the bivector valued conjugate Poisson kernel which takes the following forms

$$h_Q(\mathbf{x}) = h_{Q1}(\mathbf{x}) + h_{Q2}(\mathbf{x}) = -\frac{x\mathbf{e}_{31}}{2\pi(|\mathbf{x} + s\mathbf{e}_3|)^3} + \frac{y\mathbf{e}_{23}}{2\pi(|\mathbf{x} + s\mathbf{e}_3|)^3} = \frac{x\mathbf{e}_3}{2\pi(|\mathbf{x} + s\mathbf{e}_3|)^3} \tag{2.40}$$

and

$$\mathcal{F}\{h_Q(\mathbf{x})\} = \frac{\mathbf{u}}{|\mathbf{u}|}I_2^{-1}\exp(-2\pi|\mathbf{u}|s) \tag{2.41}$$

Fig. 2.2 illustrates the Poisson kernel and its harmonic conjugates. Combining the Poisson scale-space with its harmonic conjugates yields the monogenic scale-space [15], which can be visualized as shown in Fig. 2.3. When the scale parameter is set to zero, the
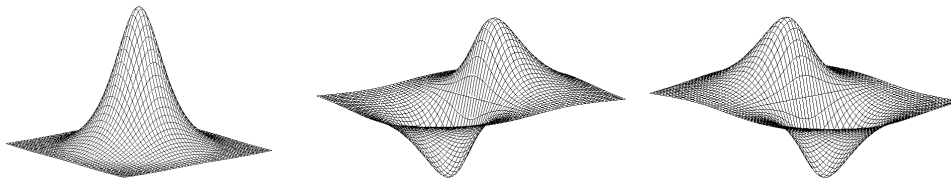
Fig. 2.2: From left to right: the Poisson kernel (h_P) and the two components of the conjugate Poisson kernel (h_{Q1} and h_{Q2}). Note that the two components of the conjugate Poisson kernel constitute one single isotropic operator.
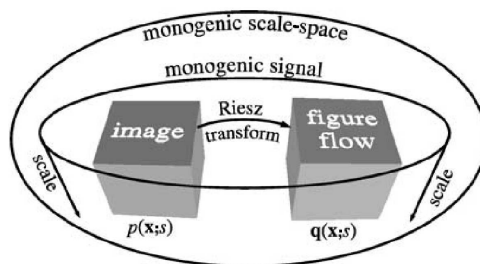

Fig. 2.3: The structure of the monogenic scale-space [15].

monogenic signal is obtained. From an alternative point of view, the monogenic scale-space can also be built by the monogenic signals at all scales, where the monogenic signals are formed by the smoothed image signals and their Riesz transformed results, i.e. the figure flows. In the monogenic scale-space, the figure flow and the smoothed signal are in quadrature phase relation at each scale. As in the case of the well known difference of Gaussian (DOG) bandpass filter, it is also possible to build up two bandpass filters in the presented framework. They are the difference of Poisson (DOP) filter and the difference of conjugate Poisson (DOCP) filter. Since the DOCP consists of two components, DOP and DOCP together form a Riesz triplet [10].

In the monogenic scale-space, expressions for the local amplitude $A_M(\mathbf{x}; s)$ and local phase $\Phi(\mathbf{x}; s)$ have to be generalized accordingly as

$$A_M(\mathbf{x}; s) = \sqrt{p(\mathbf{x}; s)^2 + |\mathbf{q}(\mathbf{x}; s)|^2} \tag{2.42}$$

$$\Phi_M(\mathbf{x}; s) = \frac{\mathbf{q}(\mathbf{x}; s)}{|\mathbf{q}(\mathbf{x}; s)|} \arctan\left(\frac{|\mathbf{q}(\mathbf{x}; s)|}{p(\mathbf{x}; s)}\right) \tag{2.43}$$

The monogenic scale-space is an interesting alternative to the Gaussian scale-space. The unique advantage of the monogenic scale-space, compared with that of the Gaussian scale-space, is the figure flow being in quadrature phase relation to the image at each scale. Therefore, the monogenic scale-space is superior to the Gaussian scale-space if a quadrature relation concept is required [15].

3. SIGNAL MODELING FOR TWO-DIMENSIONAL IMAGE STRUCTURES

So far, we understood that the monogenic signal is derived from the monogenic extension of a scalar field. However, it is restricted to model only the i1D signals because only a minimum of information, i.e. the scalar value $f(x)$, is taken into consideration. If 2D images are interpreted as surfaces in $\mathbb{R}^3$, the first and second order fundamental theorems of differential geometry would deliver the most general local signal model in the classic framework. We will associate a curvature tensor instead of a scalar value to a location of interest. This results in a useful signal model for 2D image structures. For the moment we are neglecting the metric tensor. Hence, our operators for local signal analysis will be rotation invariant.

The proposed model can be regarded as the monogenic extension of the curvature tensor. Motivated from the differential geometry, this curvature tensor can be constructed. Therefore, a brief introduction to the differential geometry is given.

3.1 Basic concepts of differential geometry

Differential geometry [7] is a well known methodology in the disciplines like physics, mechanical engineering and topography. Classical differential geometry deals with the mathematical description of curves and surfaces. In image processing field, Koenderink and van Doorn [25, 26] have introduced methods from differential geometry to analyze the local properties of signals. In such case, two dimensional intensity data can be represented as surfaces in 3D Euclidean space. Such surfaces in geometrical terms can be written as Monge patches of the form

$$\mathbf{x} + \mathbf{f}(\mathbf{x}) = x\mathbf{e}_1 + y\mathbf{e}_2 + f(x, y)\mathbf{e}_3 \qquad (3.1)$$

This notation of a surface is the most simple one for considerations in the framework of differential geometry because it enables to express the mentioned tensors with entries built from first and second order differentials of the image functions. In the following, we will introduce basic concepts of differential geometry and the general 2D signal model in an algebraic framework with more powerful geometric meanings than $\mathbb{R}_3$. Because we are interested in a tensor representation of the image signal, our model will thus be represented in the matrix geometric algebra $M(2, \mathbb{R}_3)$ which results from the tensor product $\mathbb{R}_3 \times \mathbb{R}_3$.

The matrix geometric algebra $M(2, \mathbb{R}_3)$, see [38], is the geometric algebra of 2×2 matrices with entities in $\mathbb{R}_3$. For example, a general element p in this matrix geometric algebra can be written as

$$p = \begin{bmatrix} a & b \\ c & d \end{bmatrix} \tag{3.2}$$

where $p \in M(2, \mathbb{R}_3)$ and a, b, c, $d \in \mathbb{R}_3$. Addition and multiplication of matrices in $M(2, \mathbb{R}_3)$ is the usual matrix addition and multiplication. The trace of this representation is

$$\text{trace}_M(p) = \text{trace} \begin{bmatrix} a & b \\ c & d \end{bmatrix} = a + d \tag{3.3}$$

and the corresponding determinant reads

$$\det_M(p) = \det_M \begin{bmatrix} a & b \\ c & d \end{bmatrix} = a\bar{a}d\bar{d} + b\bar{b}c\bar{c} - (\bar{a}b\bar{d}c + \bar{c}d\bar{b}a) \tag{3.4}$$

where $\bar{a}$, $\bar{b}$, $\bar{c}$ and $\bar{d}$ are the conjugations of a, b, c and d, respectively, see Eq. (2.9).

The primary first order differential quantity for an image, represented by the vector field $\mathbf{f}$, is the gradient defined as

$$\nabla \mathbf{f} = \mathbf{e}_1 \frac{\partial}{\partial x} f(x, y) \mathbf{e}_3 + \mathbf{e}_2 \frac{\partial}{\partial y} f(x, y) \mathbf{e}_3 = f_x \mathbf{e}_{13} + f_y \mathbf{e}_{23} \tag{3.5}$$

For second order geometry, the matrix of second order derivatives or Hessian H is given by

$$H_M = \begin{bmatrix} \frac{\partial^2}{\partial x^2} \mathbf{f} & \frac{\partial^2}{\partial x \partial y} \mathbf{f} \\ \frac{\partial^2}{\partial y \partial x} \mathbf{f} & \frac{\partial^2}{\partial y^2} \mathbf{f} \end{bmatrix} = \begin{bmatrix} \mathbf{e}_1 \frac{\partial}{\partial x} f_x \mathbf{e}_{13} & \mathbf{e}_2 \frac{\partial}{\partial y} f_x \mathbf{e}_{13} \\ \mathbf{e}_1 \frac{\partial}{\partial x} f_y \mathbf{e}_{23} & \mathbf{e}_2 \frac{\partial}{\partial y} f_y \mathbf{e}_{23} \end{bmatrix} = \begin{bmatrix} f_{xx} \mathbf{e}_3 & -f_{xy} \mathbf{e}_{123} \\ f_{xy} \mathbf{e}_{123} & f_{yy} \mathbf{e}_3 \end{bmatrix} \tag{3.6}$$

The Hessian matrix is related to the curvature tensor, which describes the local deviation of the signal $\mathbf{f}$ from the tangent plane of the surface.

According to the derivative theorem of Fourier theory [35, 2], in the spectral domain, the second derivative of $\mathbf{f}$ with respect to the x axis is given by

$$\mathcal{F}\{f_{xx} \mathbf{e}_3\} = -4\pi^2 \rho^2 \cos^2(\alpha) \mathbf{F} = -4\pi^2 \rho^2 \frac{1 + \cos(2\alpha)}{2} \mathbf{F} \tag{3.7}$$

where $\mathbf{F}$ denotes the Fourier transform of the original signal $\mathbf{f} = f(x, y) \mathbf{e}_3$. Analogously, the other second order derivatives are obtained as

$$\mathcal{F}\{f_{xy} \mathbf{e}_{123}\} = -4\pi^2 \rho^2 \cos(\alpha) \sin(\alpha) \mathbf{e}_{12} \mathbf{F} = -4\pi^2 \rho^2 \frac{\sin(2\alpha)}{2} \mathbf{e}_{12} \mathbf{F} \tag{3.8}$$

$$\mathcal{F}\{f_{yy} \mathbf{e}_3\} = -4\pi^2 \rho^2 \sin^2(\alpha) \mathbf{F} = -4\pi^2 \rho^2 \frac{1 - \cos(2\alpha)}{2} \mathbf{F} \tag{3.9}$$

Hence, in the spectral domain, the Hessian matrix reads

$$\mathcal{F}\{H_M\} = \begin{bmatrix} -4\pi^2 \rho^2 \frac{1 + \cos(2\alpha)}{2} \mathbf{F} & (4\pi^2 \rho^2 \frac{\sin(2\alpha)}{2} \mathbf{F}) \mathbf{e}_{12} \\ (-4\pi^2 \rho^2 \frac{\sin(2\alpha)}{2} \mathbf{F}) \mathbf{e}_{12} & -4\pi^2 \rho^2 \frac{1 - \cos(2\alpha)}{2} \mathbf{F} \end{bmatrix} \tag{3.10}$$

Tab. 3.1: Surface type classification based on Gaussian curvature and mean curvature

Surface type	M(Mean Curvature)	K(Gaussian Curvature)
Elliptic (i2D)		$K > 0$
Hyperbolic (i2D)		$K < 0$
Parabolic (i1D)	$\lvert M \rvert \neq 0$	$K = 0$
Planar (i0D)	$\lvert M \rvert = 0$	$K = 0$

According to Eq. (3.4), the determinant of the Hessian in this algebraic framework is obtained as

$$\det{}_M(H_M) = \left[(f_{xx}\mathbf{e}_3)(f_{yy}\mathbf{e}_3) - (-f_{xy}\mathbf{e}_{123})(f_{xy}\mathbf{e}_{123})\right]^2 = \left[f_{xx}f_{yy} - f_{xy}^2\right]^2 \tag{3.11}$$

This determinant is identical to the square of the classic Hessian determinant in the vector algebra. In general, the determinant computation of the algebra $M(2, \mathbb{R}_3)$ can not be reduced to the original definition in the vector algebra. However, in the current case, due to the particular basis elements, the original definition of the determinant can still be used, see Appendix for details. Hence, the determinant of the Hessian is reformulated as

$$\det{}_R(H_M) = (f_{xx}\mathbf{e}_3)(f_{yy}\mathbf{e}_3) - (-f_{xy}\mathbf{e}_{123})(f_{xy}\mathbf{e}_{123}) = f_{xx}f_{yy} - f_{xy}^2 = \lambda_1\lambda_2 \tag{3.12}$$

where λ_1 and λ_2 are two eigenvalues of the real valued Hessian matrix, which represent the principal curvatures. Thus, the Gaussian curvature K can be defined as

$$K = \det{}_R(H_M) \tag{3.13}$$

or

$$K^2 = \det{}_M(H_M) \tag{3.14}$$

The mean curvature M, obtained from the trace of the algebraically embedded Hessian matrix, takes the following form

$$M = \frac{1}{2}\text{trace}_M(H_M) = \frac{1}{2}(f_{xx}\mathbf{e}_3 + f_{yy}\mathbf{e}_3) = \frac{1}{2}(\lambda_1 + \lambda_2)\mathbf{e}_3 \tag{3.15}$$

Hence, both the Gaussian curvature and the mean curvature give rise to a rotation invariant local analysis of second order features. Combining the Gaussian curvature and mean curvature, a complete classification of the local structure into the types i2D (elliptic and hyperbolic regions), i1D (parabolic region) and i0D (planar region) in principle can be done, see table 3.1.

3.2   Monogenic extension of the curvature tensor

In order to build a general model for 2D structures with phase information contained, we follow the ideas of deriving the analytic or monogenic signal from a real valued 1D or 2D image signal. The holomorphic (1D) or monogenic (2D) completion of the

signal results in an additional component which is in quadrature phase relation to the original signal. For a 2D image, every image point is now associated with a curvature tensor which is related to the Hessian matrix. It is necessary to find a conjugate matrix with quadrature phase relationship to the curvature tensor. In the following, we will introduce the general signal model based on 2D spherical harmonics.

As analyzed before, the Hessian matrix contains curvature information. Based on it, i0D, i1D and i2D structures can be easily separated. It is obvious that angular parts of the derivatives are related to spherical harmonics of even orders 0 and 2, see equations (3.7) to (3.10). These harmonics represent the even information of 2D structures. Therefore, we are motivated to construct a tensor T_e, which is related to the Hessian matrix, for the signal modeling. We will call T_e as the curvature tensor, although it is different to the curvature tensor of the second fundamental form of the differential geometry. This curvature tensor indicates the even information of 2D structures and is obtained from a tensor-valued filter H_e in the frequency domain, i.e. $T_e = \mathcal{F}^{-1}\{H_e \times_\tau \mathbf{F}\}$, where $\mathcal{F}^{-1}$ means the inverse Fourier transform and $\times_\tau$ indicates the geometric product between all elements of H_e and $\mathbf{F}$. Since the original 2D signal $f(x,y)$ is embedded as an $\mathbf{e}_3$-valued signal, the tensor-valued filter H_e, called the even Hessian operator, thus takes the following form

$$
\begin{aligned}
H_e &= \frac{1}{2}\begin{bmatrix} H_0 + \langle H_2 \rangle_0 & -\langle H_2 \rangle_2 \\ \langle H_2 \rangle_2 & H_0 - \langle H_2 \rangle_0 \end{bmatrix} \\
&= \frac{1}{2}\begin{bmatrix} 1 + \cos(2\alpha) & -\sin(2\alpha)\mathbf{e}_{12} \\ \sin(2\alpha)\mathbf{e}_{12} & 1 - \cos(2\alpha) \end{bmatrix} = \begin{bmatrix} \cos^2(\alpha) & -\frac{1}{2}\sin(2\alpha)\mathbf{e}_{12} \\ \frac{1}{2}\sin(2\alpha)\mathbf{e}_{12} & \sin^2(\alpha) \end{bmatrix}
\end{aligned}
\tag{3.16}
$$

The entities of H_e are obtained from Eq. (3.10). For the convenience of analysis, the radial factors are ignored.

In this filter, the two elements $\cos^2(\alpha)$ and $\sin^2(\alpha)$ can be considered as two angular windowing functions which are the same as those of the orientation tensor in [21]. From them, two perpendicular i1D components of the 2D image, oriented along the $\mathbf{e}_1$ and $\mathbf{e}_2$ coordinates, can be obtained. The other component of the filter is also the combination of two angular windowing functions, i.e. $\frac{1}{2}\sin(2\alpha) = \frac{1}{2}(\cos^2(\alpha - \frac{\pi}{4}) - \sin^2(\alpha - \frac{\pi}{4}))$. These two angular windowing functions yield again two i1D components of the 2D image, which are oriented along the diagonals of the plane spanned by $\mathbf{e}_1$ and $\mathbf{e}_2$. These four angular windowing functions, shown in Fig. 3.1, can also be considered as four differently oriented filters, which are basis functions to steer a detector for i1D structures [19]. They make sure that i1D components along different orientations are extracted, see Fig. 3.2. Consequently, the even Hessian operator H_e enables the extraction of four differently oriented i1D components of the 2D image. Hence, the superimpose of these four basis i1D signals will result in a rotation-invariant extraction of any arbitrary i1D signal.

The Riesz transform [14] is able to evaluate the corresponding conjugate information of the i1D signal, which is in quadrature phase relation with the i1D signal. Therefore, the odd representation of the curvature tensor, called the conjugate curvature tensor T_o, is obtained by employing the first order spherical harmonic h_1 to elements of T_e, which equals the Riesz transform of the curvature tensor T_e. Besides, the conjugate curvature
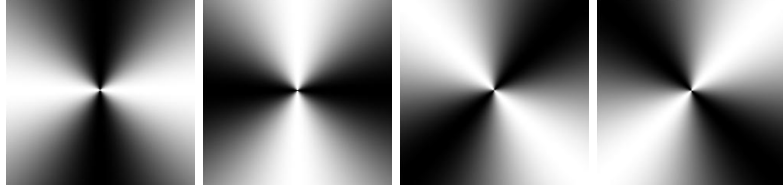
Fig. 3.1: From left to right are the angular windowing functions of $\cos^2(\alpha)$, $\sin^2(\alpha)$, $\cos^2(\alpha - \frac{\pi}{4})$ and $\sin^2(\alpha - \frac{\pi}{4})$. White indicates positive one and black represents zero.
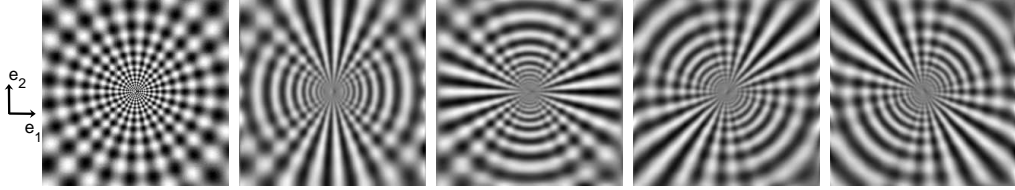

Fig. 3.2: From left to right are the test image, i1D signals result from the angular windowing functions of $\cos^2(\alpha)$, $\cos^2(\alpha - \frac{\pi}{4})$, $\sin^2(\alpha)$ and $\sin^2(\alpha - \frac{\pi}{4})$, respectively.

tensor T_o results also from a tensor-valued filter H_o, called the odd Hessian operator.

$$T_o = h_1 *_\tau T_e = \mathcal{F}^{-1}\{H_o \times_\tau \mathbf{F}\} \tag{3.17}$$

where $*_\tau$ represents the convolution of all elements of T_e with h_1. The odd Hessian operator H_o equals the Riesz transform of the even Hessian operator, i.e. $H_o = H_1 \times_\tau H_e$. In the spectral domain, the odd Hessian operator thus takes the following form

$$H_o \equiv \begin{bmatrix} H_{o11} & H_{o12} \\ H_{o21} & H_{o22} \end{bmatrix} = \frac{1}{2}\begin{bmatrix} H_1(H_0 + \langle H_2 \rangle_0) & H_1(-\langle H_2 \rangle_2) \\ H_1(\langle H_2 \rangle_2) & H_1(H_0 - \langle H_2 \rangle_0) \end{bmatrix} \tag{3.18}$$

with

$$H_{o11} = (\cos(\alpha) + \sin(\alpha)\mathbf{e}_{12})(\cos^2(\alpha)) \tag{3.19}$$
$$= \frac{1}{4}[(3\cos(\alpha) + \cos(3\alpha)) + (\sin(\alpha) + \sin(3\alpha))\mathbf{e}_{12}]$$
$$H_{o21} = -H_{o12} = (\cos(\alpha) + \sin(\alpha)\mathbf{e}_{12})(\frac{1}{2}\sin(2\alpha)\mathbf{e}_{12}) \tag{3.20}$$
$$= \frac{1}{4}[(\cos(\alpha) - \cos(3\alpha)) + (\sin(\alpha) + \sin(3\alpha))\mathbf{e}_{12}]$$
$$H_{o22} = (\cos(\alpha) + \sin(\alpha)\mathbf{e}_{12})(\sin^2(\alpha)) \tag{3.21}$$
$$= \frac{1}{4}[(\cos(\alpha) - \cos(3\alpha)) + (3\sin(\alpha) - \sin(3\alpha))\mathbf{e}_{12}]$$

It is obvious that this tensor-valued filter consists of odd order spherical harmonics. Hence, the Riesz transform of the curvature tensor T_e gives its corresponding odd representation T_o. Combing the curvature tensor and its conjugate representation forms the general signal model of local 2D image structures,

$$T(\mathbf{x}) = T_e(\mathbf{x}) + T_o(\mathbf{x}) \tag{3.22}$$

This signal model can also be regarded as the monogenic extension of the curvature tensor. Hence, it is called the monogenic curvature tensor.

In fact, the monogenic curvature tensor is an element of $M(2, \mathbb{R}_3)$ with monogenic entries. This representation is much more powerful than the monogenic signal. There for each pixel a real signal is extended to a Clifford valued signal. In our case, a Clifford valued tensor representation is gained with quadrature relations in each element of the tensor. There are different ways of evaluating the monogenic curvature tensor. One way is to evaluate the quadrature relationship of the tensor pair (T_e, T_o) separately, the other way is to evaluate the quadrature relation of the elements of $T = T_e + T_o$. We will present in this paper the first way.

3.3 Local representations for i1D and i2D image structures

Analogous with the real valued differential geometry approach, in our Clifford valued approach 2D image structures can be classified by computing the Gaussian curvature and the mean curvature of the tensor pair T_e and T_o, see also table 3.1. Since the non-zero Gaussian curvature indicates the existence of i2D structure, the even and odd parts of i2D structures are correspondingly obtained according to Eq. (3.13). The even part of i2D structures reads

$$
\begin{aligned}
\mathbf{d}_e &= \det{}_R(T_e)\mathbf{e}_3 = (T_{e11}T_{e22} - T_{e12}T_{e21})\mathbf{e}_3 & (3.23)\\
&= \mathcal{F}^{-1}\left\{\left[\left(\frac{H_0 + \langle H_2\rangle_0}{2}\mathbf{F}\right) * \left(\frac{H_0 - \langle H_2\rangle_0}{2}\mathbf{F}\right) - \left(\frac{\langle H_2\rangle_2}{2}\mathbf{F}\right) * \left(\frac{-\langle H_2\rangle_2}{2}\mathbf{F}\right)\right]\mathbf{e}_3\right\}\\
&= \mathcal{F}^{-1}\left\{\left[\left(\frac{1 + \cos(2\alpha)}{2}\mathbf{F}\right) * \left(\frac{1 - \cos(2\alpha)}{2}\mathbf{F}\right) - \left(\frac{\sin(2\alpha)}{2}\mathbf{F}\right) * \left(\frac{-\sin(2\alpha)}{2}\mathbf{F}\right)\right]\mathbf{e}_3\right\}\\
&= A\mathbf{e}_3
\end{aligned}
$$

where T_{eij}, $i, j = 1, 2$ are the corresponding components of the curvature tensor T_e. Because $\det{}_R(T_e)$ is scalar valued, similar as the monogenic signal, the even part of i2D structures is embedded as the $\mathbf{e}_3$ component in the 3D Euclidean space. The odd part of i2D structures is given by

$$
\begin{aligned}
\mathbf{d}_o &= \mathbf{e}_1\det{}_R(T_o) = \mathbf{e}_1(T_{o11}T_{o22} - T_{o12}T_{o21}) & (3.24)\\
&= \mathcal{F}^{-1}\left\{\mathbf{e}_1\left[\left(\frac{H_1(H_0 + \langle H_2\rangle_0)}{2}\mathbf{F}\right) * \left(\frac{H_1(H_0 - \langle H_2\rangle_0)}{2}\mathbf{F}\right)\right.\right. & (3.25)\\
&\qquad\left.\left. - \left(\frac{H_1(\langle H_2\rangle_2)}{2}\mathbf{F}\right) * \left(\frac{-H_1(\langle H_2\rangle_2)}{2}\mathbf{F}\right)\right]\right\}\\
&= B\mathbf{e}_1 + C\mathbf{e}_2
\end{aligned}
$$

where T_{oij}, $i, j = 1, 2$ are the corresponding components of the conjugate curvature tensor T_o. Because $\det{}_R(T_o)$ is spinor valued, i.e. $\det{}_R(T_o) \in span\{1, \mathbf{e}_{12}\}$, by multiplying the $\mathbf{e}_1$ basis vector from the left, $\mathbf{d}_o$ takes a vector valued representation. A local representation for i2D structures is obtained by combining the even and odd parts of i2D

structures. This local representation for i2D structures is called the monogenic curvature signal and it takes the following form

$$\mathbf{f}_{i2D} = \mathbf{d}_e + \mathbf{d}_o = A\mathbf{e}_3 + B\mathbf{e}_1 + C\mathbf{e}_2 \tag{3.26}$$

The original signal $\mathbf{f}(\mathbf{x}), \mathbf{x} \in \mathbb{R}^2$ is thus mapped to $\mathbf{f}_{i2D}(\mathbf{x}), \mathbf{x} \in \mathbb{R}^3$ as a local representation of i2D signals. The monogenic curvature signal can be considered as a monogenic representation of the Gaussian curvature in real valued differential geometry.

The parabolic and planar surface patches, corresponding to i1D and i0D structures, have zero Gaussian curvatures. In order to separate them with each other, the trace of the tensor pair T_e and T_o is computed. Non-zero trace illustrates the existence of i1D structure. Therefore, the combination of traces of T_e and T_o can be considered as the local representation of i1D structures. According to the combination and certain embedding, this representation is obtained as

$$\begin{aligned} \mathbf{f}_{i1D} &= \text{trace}(T_e) + \text{trace}(T_o)\mathbf{e}_2 = \mathcal{F}^{-1}\left\{\text{trace}(H_e \times_\tau \mathbf{F}) + \text{trace}(H_o \times_\tau \mathbf{F})\mathbf{e}_2\right\} \\ &= \mathcal{F}^{-1}\left\{[\text{trace}(H_e) + (-\mathbf{e}_2)\text{trace}(H_o)]\mathbf{F}\right\} \end{aligned} \tag{3.27}$$

with

$$\begin{aligned} \text{trace}(H_e) + (-\mathbf{e}_2)\text{trace}(H_o) &= 1 + (-\mathbf{e}_2)H_1 = 1 + (-\mathbf{e}_2)(\cos(\alpha) + \sin(\alpha)\mathbf{e}_{12}) \\ &= 1 + \cos(\alpha)(-\mathbf{e}_2) + \sin(\alpha)\mathbf{e}_1 = 1 + H_R \end{aligned} \tag{3.28}$$

where H_R refers to the Riesz kernel in the spectral domain, see Eq. (2.32). Plugging Eq. (3.28) into Eq. (3.27), we will get the i1D structure representation as

$$\begin{aligned} \mathbf{f}_{i1D} &= \mathcal{F}^{-1}\left\{[\text{trace}(H_e) + (-\mathbf{e}_2)\text{trace}(H_o)]\mathbf{F}\right\} \\ &= \mathcal{F}^{-1}\left\{(1 + H_R)\mathbf{F}\right\} = \mathbf{f} + h_R * \mathbf{f} = f_3(\mathbf{x})\mathbf{e}_3 + f_1(\mathbf{x})\mathbf{e}_1 + f_2(\mathbf{x})\mathbf{e}_2 \end{aligned} \tag{3.29}$$

where h_R is the spatial representation of the Riesz kernel and $\mathbf{f}$ refers to the $\mathbf{e}_3$ valued original signal. The obtained Eq. (3.29) is identical to Eq. (2.13), which indicates that the local representation for i1D structures, obtained from the general signal model, is the combination of the original signal and its Riesz transform. This means that the derived i1D structure representation is just the monogenic signal as proposed in [14]. Hence, the proposed signal model includes the monogenic signal as a special case, which is a monogenic measure of the mean curvature. In addition to this, it constitutes also the local representation for i2D structure. Therefore, the signal model is a general representation for 2D structures of any intrinsic dimension.

4. INTERPRETATION OF THE MONOGENIC CURVATURE SIGNAL

Because the monogenic signal has been discussed in [14] in detail, we are more interested in the interpretation of the i2D structure representation, i.e. the monogenic curvature signal.

4.1 Geometric model and feature extraction

In the light of the introduction in Section 2.1, local features of the monogenic curvature signal can be defined using the logarithm of $\mathbb{R}_3^+$. The spinor field which maps the $\mathbf{e}_3$ basis vector to the monogenic curvature signal $\mathbf{f}_{i2D}$ is given by $\mathbf{e}_3\mathbf{f}_{i2D}$. According to Eq. (2.15) and Eq. (2.16), the local amplitude $A(\mathbf{x})$ and local phase representation $\Phi(\mathbf{x})$ are obtained as

$$A(\mathbf{x}) = |\mathbf{f}_{i2D}(\mathbf{x})| = \exp(\log(|\mathbf{e}_3\mathbf{f}_{i2D}(\mathbf{x})|)) = \exp(\langle\log(\mathbf{e}_3\mathbf{f}_{i2D}(\mathbf{x}))\rangle_0) \tag{4.1}$$

$$\Phi(\mathbf{x}) = \arg(\mathbf{f}_{i2D}(\mathbf{x})) = \langle\log(\mathbf{e}_3\mathbf{f}_{i2D}(\mathbf{x}))\rangle_2 = \frac{\langle\mathbf{e}_3\mathbf{f}_{i2D}(\mathbf{x})\rangle_2}{|\langle\mathbf{e}_3\mathbf{f}_{i2D}(\mathbf{x})\rangle_2|}\mathrm{atan}\left(\frac{|\langle\mathbf{e}_3\mathbf{f}_{i2D}(\mathbf{x})\rangle_2|}{\langle\mathbf{e}_3\mathbf{f}_{i2D}(\mathbf{x})\rangle_0}\right) \tag{4.2}$$

where $\arg(\cdot)$ denotes the argument of the expression and $\mathrm{atan}(\cdot) \in [0, \pi)$. As the bivector part of the logarithm of the spinor field $\mathbf{e}_3\mathbf{f}_{i2D}$, this local phase representation describes a rotation from the $\mathbf{e}_3$ axis by a phase angle φ in the oriented complex plane spanned by $\mathbf{f}_{i2D}$ and $\mathbf{e}_3$, i.e. $\mathbf{f}_{i2D} \wedge \mathbf{e}_3$. The orientation of this phase plane indicates the local main orientation. Therefore, the local phase representation of the monogenic curvature signal combines local phase and local orientation of i2D structures, just as in the case of the monogenic signal for i1D structures. Since the local phase representation $\Phi(\mathbf{x})$ is a bivector, its dual in $\mathbb{R}_3$ is a rotation vector that can be defined as

$$\mathbf{r}(\mathbf{x}) = (\Phi(\mathbf{x}))^* = \langle\log(\mathbf{e}_3\mathbf{f}_{i2D}(\mathbf{x}))\rangle_2^* \tag{4.3}$$

The rotation vector $\mathbf{r}$ is orthogonal to the local orientation. The length of the rotation vector $|\mathbf{r}|$ indicates the phase angle φ of the i2D structure and its direction illustrates the rotation axis. According to the proposed algebraic embedding, a geometric model for the monogenic curvature signal can be visualized as shown in figure 4.1. The geometric model is an ellipsoid, which looks very similar to that of the monogenic signal. However, each axis encodes totally different meaning. The even part of the i2D structure is encoded within the $\mathbf{e}_3$ axis, and the odd part is encoded within the $\mathbf{e}_1$ and $\mathbf{e}_2$ axes.
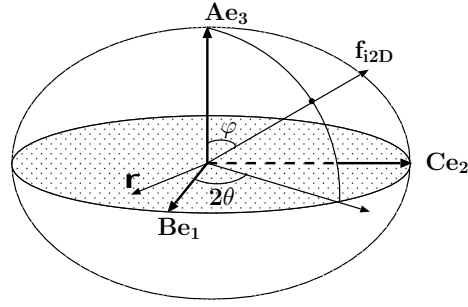
Fig. 4.1: The geometric model for the monogenic curvature signal. Here, $A\mathbf{e}_3$ indicates the even information of the i2D structure, $B\mathbf{e}_1$ and $C\mathbf{e}_2$ are the two components of the odd part. The phase is represented by φ, 2θ denotes the main orientation in terms of double angle representation, $\mathbf{r}$ indicates the rotation vector.

The angle φ represents the phase and 2θ is the main orientation in a double angle representation form. The rotation vector $\mathbf{r}$ lies in the plane orthogonal to $\mathbf{e}_3$. Combining the local amplitude and local phase representation, the monogenic curvature signal for i2D structures can be reconstructed as

$$\mathbf{f}_{i2D} = |\mathbf{f}_{i2D}|\exp\left(\arg\left(\mathbf{f}_{i2D}\right)\right) \tag{4.4}$$

Having a definition for the i2D local phase, we recognize that the local phase representation contains additional geometric information, i.e. local orientation. Since local amplitude, local phase and local orientation are orthogonal to each other, the monogenic curvature signal performs a split of identity.

From an alternative point of view, local amplitude, phase and orientation can also be obtained according to the relationship of the even and odd components in spherical coordinates. The local amplitude is computed as

$$|\mathbf{f}_{i2D}| = \sqrt{A^2 + B^2 + C^2} \tag{4.5}$$

The local main orientation is given by

$$\theta = \frac{1}{2}\text{atan2}(B, C) \qquad \theta \in (-\frac{\pi}{2}, \frac{\pi}{2}] \tag{4.6}$$

where $\text{atan2}(\cdot) \in (-\pi, \pi]$. And the local phase reads

$$\varphi = \text{atan2}\left(\text{sign}(B\mathbf{e}_1 + C\mathbf{e}_2)|B\mathbf{e}_1 + C\mathbf{e}_2|, A\right) \qquad \varphi \in (-\pi, \pi] \tag{4.7}$$

Fig. 4.2 illustrates bandpassed local features extracted from the monogenic curvature signal. A synthetic image which consists of a superposition of an angular and a radial modulation is used as the test image. The blobs in this test image are considered as i2D structures. The energy output of the monogenic curvature signal, i.e. $\mathbf{d}_e^2 + \mathbf{d}_o^2$, can be regarded as i2D structure strength to detect points of interest. Besides, it also illustrates the rotation invariance property of the monogenic curvature signal. The even and odd outputs also indicate the existence of i2D structures. Local main orientation
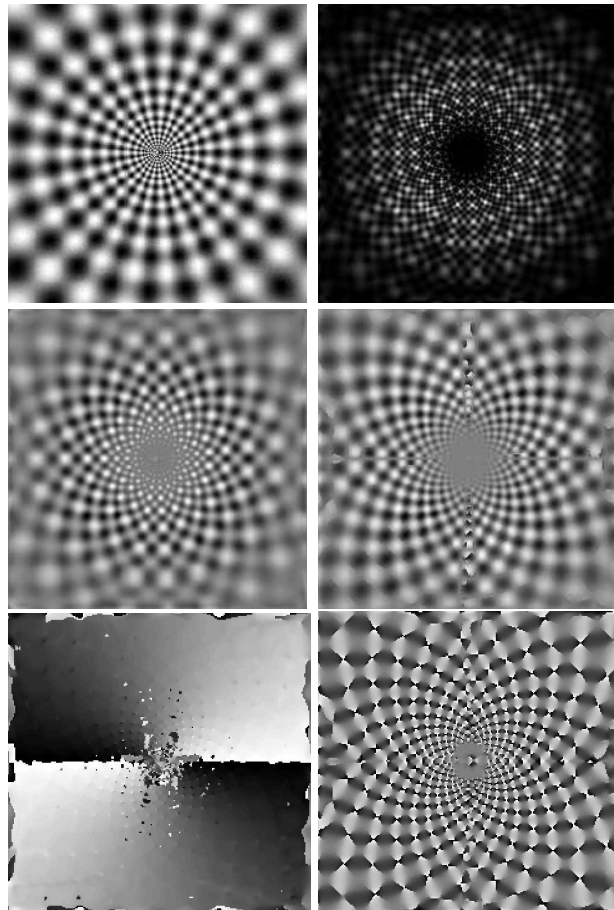
Fig. 4.2: Bandpassed local features. Top row: from left to right are the original image and the energy output of the monogenic curvature signal. Middle row: even and odd parts of the monogenic curvature signal. Bottom row: the estimated main orientation and phase.
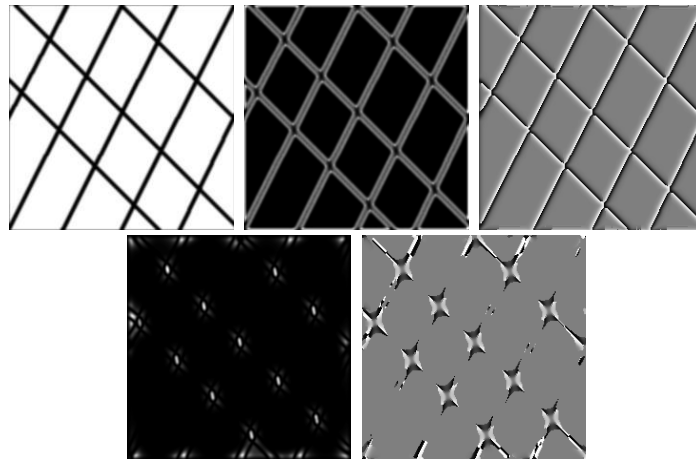
Fig. 4.3: Top row: test image, the energy of the monogenic signal and its phase. Bottom row: Energy and phase of the monogenic curvature signal.
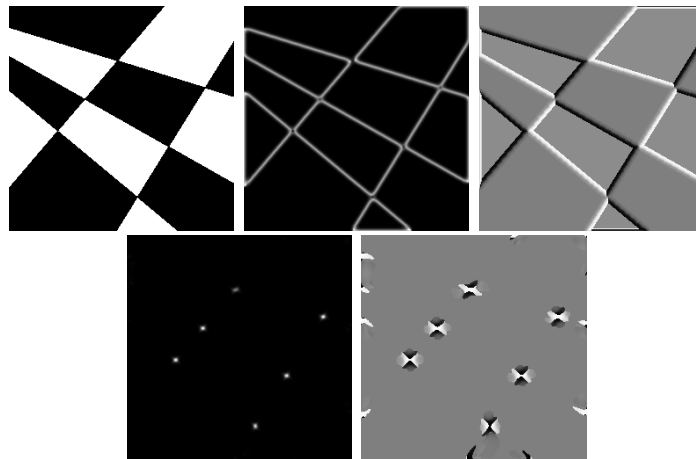

Fig. 4.4: Top row: test image, the energy of the monogenic signal and its phase. Bottom row: Energy and phase of the monogenic curvature signal.

of the monogenic curvature signal denotes the main orientation of the i2D structure. Its minor orientation is simply perpendicular to the main orientation. Local phase contains the structure information. At the positions where the main orientation and the minor orientation wrap form zero to π, the estimated phase is inverted. This is called the orientation-phase wrapping.

To show the difference between the monogenic signal and the monogenic curvature signal, some experimental results are given in Fig. 4.3 and Fig. 4.4. Two patterns as the line and edge like intersection are employed as test images. Local energy output and phase information from the monogenic signal and the monogenic curvature signal are extracted, respectively. These results indicate that the monogenic signal enables the feature estimation of i1D signals, however, it delivers no information for the i2D part of the original signal. The monogenic curvature signal is in contrast gives access to local feature evaluation of i2D structures.

4.2 Properties of the monogenic curvature signal

According to Eq. (3.23), in the spectral domain, the even part of the monogenic curvature signal $\mathbf{d}_e$ can be interpreted as

$$\mathcal{F}\{\mathbf{d}_e\} = \mathcal{F}\{\det{}_R(T_e)\mathbf{e}_3\} = ((H_{e11}(\alpha)H_{DOP}(\rho;s)\mathbf{F}) * (H_{e22}(\alpha)H_{DOP}(\rho;s)\mathbf{F})$$
$$-(H_{e12}(\alpha)H_{DOP}(\rho;s)\mathbf{F}) * (H_{e21}(\alpha)H_{DOP}(\rho;s)\mathbf{F}))\mathbf{e}_3 \qquad (4.8)$$

where $H_{eij}(\alpha)$, $i,j = 1,2$ are the corresponding components in the tensor-valued even Hessian operator H_e. Only if Eq. (4.8) delivers a non-zero output, the existence of i2D structures is indicated. For i0D and i1D structures, the result of Eq. (4.8) is zero. The i1D signals in the frequency domain are straight lines through the origin, therefore, the two dimensional convolutions in Eq. (4.8) can be reduced to 1D convolutions along the properly oriented axis, indicated by the fixed angle α_0. Then, Eq. (4.8) can be rewritten as

$$\mathcal{F}\{\mathbf{d}_e\} = ([H_{e11}(\alpha_0)H_{e22}(\alpha_0)]\,[(H_{DOP}(\rho;s)\mathbf{F}) * (H_{DOP}(\rho;s)\mathbf{F})] -$$
$$[H_{e12}(\alpha_0)H_{e21}(\alpha_0)]\,[(H_{DOP}(\rho;s)\mathbf{F}) * (H_{DOP}(\rho;s)\mathbf{F})])\mathbf{e}_3 \qquad (4.9)$$

To ensure $\mathcal{F}\{\mathbf{d}_e\}$ to be zero for an i1D signal, the condition should be

$$H_{e11}(\alpha_0)H_{e22}(\alpha_0) = H_{e12}(\alpha_0)H_{e21}(\alpha_0) \qquad (4.10)$$

Hence, Eq. (4.10) makes sure that the even part is selective to the i2D structures and it was called the compensation equation in [41]. In the case of monogenic curvature signal, for its even part, we have

$$H_{e11}(\alpha_0)H_{e22}(\alpha_0) = \cos^2(\alpha_0)\sin^2(\alpha_0) = \frac{1}{4}\sin(2\alpha_0) \qquad (4.11)$$

$$H_{e12}(\alpha_0)H_{e21}(\alpha_0) = \frac{1}{2}\sin(2\alpha_0)\frac{1}{2}\sin(2\alpha_0) = \frac{1}{4}\sin(2\alpha_0) \qquad (4.12)$$

Therefore, the compensation Eq. (4.10) is satisfied and can be rewritten as

$$\cos^2(\alpha_0)\sin^2(\alpha_0) = \frac{1}{2}\sin(2\alpha_0)\frac{1}{2}\sin(2\alpha_0) \qquad (4.13)$$

This equation decides that the even part of the monogenic curvature signal is selective to the i2D structure and the i1D structure can be suppressed.

Analogously, the odd part of the monogenic curvature signal $\mathbf{d}_o$ in the Fourier domain reads

$$\mathcal{F}\{\mathbf{d}_o\} = \mathcal{F}\{\mathbf{e}_1\det{}_R(T_o)\} = \mathbf{e}_1((H_{o11}(\alpha)H_{DOP}(\rho;s)\mathbf{F}) * (H_{o22}(\alpha)H_{DOP}(\rho;s)\mathbf{F})$$
$$-(H_{o12}(\alpha)H_{DOP}(\rho;s)\mathbf{F}) * (H_{o21}(\alpha)H_{DOP}(\rho;s)\mathbf{F})) \qquad (4.14)$$

In order to make sure $\mathcal{F}\{\mathbf{d}_o\}$ is zero for an i1D signal, the compensation equation for the odd part of the monogenic curvature signal with the following form should be satisfied

$$H_{o11}(\alpha_0)H_{o22}(\alpha_0) = H_{o12}(\alpha_0)H_{o21}(\alpha_0) \qquad (4.15)$$

where $H_{oij}, i, j = 1, 2$ indicates the corresponding components in the tensor-valued odd Hessian operator H_o. Hence, we are able to obtain

$$H_{o11}(\alpha_0) H_{o22}(\alpha_0) = \cos(2\alpha_0) \left[\cos^2(\alpha_0) \sin^2(\alpha_0) \right] + \qquad (4.16)$$
$$\sin(2\alpha_0) \left[\cos^2(\alpha_0) \sin^2(\alpha_0) \right] \mathbf{e}_{12}$$

$$H_{o12}(\alpha_0) H_{o21}(\alpha_0) = \cos(2\alpha_0) \left[\frac{1}{2} \sin(2\alpha_0) \frac{1}{2} \sin(2\alpha_0) \right] + \qquad (4.17)$$
$$\sin(2\alpha_0) \left[\frac{1}{2} \sin(2\alpha_0) \frac{1}{2} \sin(2\alpha_0) \right] \mathbf{e}_{12}$$

It is obvious that the compensation Eq. (4.15) is satisfied and the odd part of the monogenic curvature signal does only respond to i2D structures. Consequently, the monogenic curvature signal is regarded as local representation of i2D structures.

Since the odd part of the monogenic curvature signal has two components, the compensation of the odd part can in accordance be split into two parts, that is

$$\cos(2\alpha_0)[\cos^2(\alpha_0) \sin^2(\alpha_0)] = \cos(2\alpha_0)[\frac{1}{2} \sin(2\alpha_0) \frac{1}{2} \sin(2\alpha_0)] \qquad (4.18)$$

$$\sin(2\alpha_0)[\cos^2(\alpha_0) \sin^2(\alpha_0)]\mathbf{e}_{12} = \sin(2\alpha_0)[\frac{1}{2} \sin(2\alpha_0) \frac{1}{2} \sin(2\alpha_0)]\mathbf{e}_{12} \qquad (4.19)$$

These two parts, which are derived from $\det_R(T_o) = T_{o11} T_{o22} - T_{o12} T_{o21}$, determine the two components of the odd part $B\mathbf{e}_1$ and $C\mathbf{e}_2$, respectively. Comparing the compensation equations (4.13),(4.18) and (4.19), it is shown that the determinant of the conjugate curvature tensor T_o is obtained from the curvature tensor T_e by convolving it with the second order spherical harmonic, that is

$$\det_R(T_o) = h_2 * \det_R(T_e) \qquad (4.20)$$

Therefore, the odd part of the monogenic curvature signal $\mathbf{d}_o$ can be derived from the even part $\mathbf{d}_e$ by employing the second order spherical harmonic operator, which means

$$\mathbf{f}_{i2D} = \det(T_e)\mathbf{e}_3 + \mathbf{e}_1 \det(T_o) = \mathbf{d}_e + \mathbf{d}_o = \mathbf{d}_e + (\mathbf{e}_1 h_2 \mathbf{e}_3) * \mathbf{d}_e = A\mathbf{e}_3 + B\mathbf{e}_1 + C\mathbf{e}_2 \quad (4.21)$$

The angle between $B\mathbf{e}_1$ and $C\mathbf{e}_2$ indicates the local main orientation in a double angle representation just as in the case of the structure tensor [18, 21]. It is introduced in Section 2.3 that the odd part of the monogenic signal is obtained from the even part by employing the Riesz transform, which is basically equivalent to the first order spherical harmonic. In case of the monogenic curvature signal, we have comparable relations between the even and odd parts. Only the second order spherical harmonic occurs as a new operator which is another generalization of the Hilbert transform. This enables us to state that the Riesz transform is able to generalize the Hilbert transform with respect to i1D signals and the derived generalized Hilbert transform (the second order spherical harmonic) realizes the same with respect to i2D signals. This is valid for any dimension of the signal. Furthermore, this gives rise to the conjecture that a third order spherical

harmonic will be responsible for generalizing the Hilbert transform in the case of i3D signals in the 3D case. Recently, several types of generalized Hilbert transforms have been derived in [4, 3]. Indeed, the second order spherical harmonic belongs to one of the considered types.

According to the Parseval theorem, the energy of the odd and even parts of the monogenic curvature signal are related by

$$
\begin{aligned}
E_o &= ((\mathbf{e}_1 h_2 \mathbf{e}_3) * \mathbf{d}_e)^2 = \int\int |\mathbf{e}_1 H_2 \mathbf{e}_3 \mathbf{D}_e|^2 d\rho d\alpha \qquad (4.22) \\
&= \int\int |\cos(2\alpha)\mathbf{e}_{13} + \sin(2\alpha)\mathbf{e}_{23}|^2 |\mathbf{D}_e|^2 d\rho d\alpha \\
&= \int\int (\cos^2(2\alpha) + \sin^2(2\alpha))|\mathbf{D}_e|^2 d\rho d\alpha = E_e
\end{aligned}
$$

where $\mathbf{D}_e$ represents the Fourier transform of $\mathbf{d}_e$. It can be shown that the energy of the odd part equals that of the even part. Hence, the amplitudes of even and odd part are equivalent, i.e. $|\mathbf{d}_e| = |\mathbf{d}_o|$.

As a good local representation for the i2D signal, it requires that the monogenic curvature signal has the property of rotation invariance. To analyze this property, we should start from Eq. (3.13). Hence, the Gaussian curvature of the Hessian matrix can be rewritten as

$$
\begin{aligned}
K &= f_{xx}\mathbf{e}_3 f_{yy}\mathbf{e}_3 - (-f_{xy}\mathbf{e}_{123})(f_{xy}\mathbf{e}_{123}) \qquad (4.23) \\
&= \frac{1}{4}[(f_{xx}\mathbf{e}_3 + f_{yy}\mathbf{e}_3)^2 - ((f_{xx}\mathbf{e}_3 - f_{yy}\mathbf{e}_3)^2 + (f_{xy})^2)] \\
&= \frac{1}{4}[(\Delta\mathbf{f})^2 - \varepsilon^2]
\end{aligned}
$$

where $\Delta\mathbf{f}$ is the Laplacian of the signal and ε indicates the eccentricity. Because Eq. (4.23) must be zero for the i0D and i1D signals, the compensation equation of it now changes as

$$
(\cos^2(\alpha) + \sin^2(\alpha))^2 = \cos^2(2\alpha) + \sin^2(2\alpha) \qquad (4.24)
$$

Since i0D and i1D structures are suppressed, what left is the i2D structure. Hence, spherical harmonics which serve as the angular portions, decide the rotation invariance of the i2D structure output. As stated in Section 2.1, the amplitude of the nth order spherical harmonic is rotationally invariant. Thus, the filter response from a nth order spherical harmonic has the property of rotation invariance. Therefore, the left and right sides of Eq. (4.24) determine two isotropic operations. The Gaussian curvature of the Hessian thus can be considered as the difference of two isotropic operation outputs, which proves that the property of rotation invariance is fulfilled.

A similar analysis applies to the even part of the monogenic curvature signal, that is

$$
\begin{aligned}
\mathbf{d}_e &= (T_{e11}T_{e22} - T_{e12}T_{e21})\mathbf{e}_3 \qquad (4.25) \\
&= \frac{1}{4}\left[(T_{e11} + T_{e22})^2 - ((T_{e11} - T_{e22})^2 + T_{e12}T_{e21}))\right]\mathbf{e}_3
\end{aligned}
$$

The compensation for $\mathbf{d}_e$ now takes the same form as the compensation Eq. (4.24). Therefore, $\mathbf{d}_e$ is rotationally invariant. According to equations (4.21) and (4.22), the odd part is obtained by convolving the even part with the second order spherical harmonic and the energy of them are equivalent, therefore, the amplitude of the odd part $\mathbf{d}_o$ is also rotationally invariant.

Hence, we can conclude the properties of the monogenic curvature signal as follows

- It enables the simultaneous estimation of local amplitude, local main orientation and local phase of i2D structures.

- It is rotationally invariant and no steering is needed.

- The odd part is transformed from the even part by the second order spherical harmonic, i.e. $\mathbf{d}_o = (\mathbf{e}_1 h_2 \mathbf{e}_3) * \mathbf{d}_e$.

- The energy of the even part is equal to that of the odd part, i.e. $\mathbf{d}_e^2 = \mathbf{d}_o^2$.

- Since the local amplitude and local phase representation are independent of each other, the monogenic curvature signal fulfills the split of identity.

5. PARITY SYMMETRY ANALYSIS

5.1 Preliminaries

Parity symmetry, as an important local feature of qualitative signal analysis, is strongly related to the local phase of the signal [39]. In image processing, parity symmetry is a cue for the line-like or edge-like quality of a local image structure. Parity refers to the invariance of a process with respect to a reflection operation. It is well known that any real signal $f : \mathbb{R}^n \to \mathbb{R}$ at any location $\mathbf{x} \in \mathbb{R}^n$ can be decomposed into an even and odd part, i.e. $f(\mathbf{x}) = f_e(\mathbf{x}) + f_o(\mathbf{x})$ [21]. A real signal has even symmetry if $f(-\mathbf{x}) = f(\mathbf{x})$ and odd symmetry if $f(-\mathbf{x}) = -f(\mathbf{x})$ for all $\mathbf{x} \in \mathbb{R}^n$.

In 1D, the local phase of a signal is defined as the angular part of its analytic signal. If the local energy is zero, no phase analysis is available. Once the local energy exceeds a certain threshold, the parity symmetry would then enable a local structure analysis. The relation between the local structure and local phase is illustrated in Fig. 5.1. At a signal position with locally even symmetry, only the real valued even part of the quadrature filter matches. Thus, the phase is 0 for a peak like signal and π for a dip like signal. A similar reflection reveals the odd case for edge like signals. Only the odd, and thus the imaginary, filter component matches the signal. Therefore, the signal structure has a phase of $\frac{\pi}{2}$ for decreasing slope and $-\frac{\pi}{2}$ for increasing slope. For i1D signals, the monogenic phase also indicates the even and odd symmetry as line and edge like structures in a rotation-invariant manner. The line-like structure is even symmetric with respect to its orientation vector, hence, the odd output of the monogenic signal is zero. The edge-like structure is pure odd symmetric with respect to its orientation vector, therefore, no even output from the monogenic signal exists.

A phase concept of i2D signals has been investigated by Bülow and Sommer [6, 5].
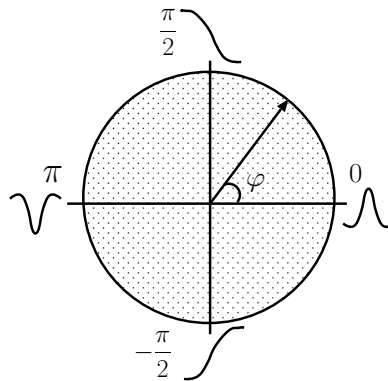

Fig. 5.1: The relation between the local signal structure and local phase in 1D case.
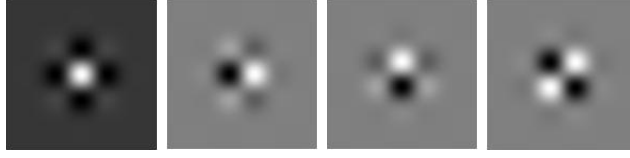
Fig. 5.2: Four components of the quaternionic Gabor filter.

In this approach, a two-dimensional signal is split into even and odd parts along the x-axis and along the y-axis, i.e. $\mathbf{f} = \mathbf{f}_{ee} + \mathbf{f}_{oe} + \mathbf{f}_{eo} + \mathbf{f}_{oo}$. Here, $\mathbf{f}_{ee}$ denotes the part of $\mathbf{f}$ that is even with respect to x and y, $\mathbf{f}_{oe}$ represents the part which is odd with respect to x and even with respect to y and so on. These four symmetries are obtained by convolving the signal with four components of a quaternionic Gabor filter which are shown in Fig. 5.2. Those four components have the even-even, odd-even, even-odd and odd-odd symmetries with respect to the coordinates. The estimated phase information can, to some extent, illustrate the intrinsic dimensionality of local structures. Unfortunately, this approach has the drawback of being not rotation invariant.

5.2 Parity symmetry of the monogenic curvature signal

The monogenic curvature signal also enables the rotation invariant extraction of a phase for i2D signals. The presented phase interpretation strongly depends on the way the monogenic curvature tensor is analyzed. Here, we study only the relations between its even and odd components. The parity symmetry involved in our case can be analyzed from the even and odd parts of the monogenic curvature signal, respectively. As indicated in Section 3, the even part is computed as,

$$\mathbf{d}_e = (T_{e11}T_{e22} - T_{e12}T_{e21})\mathbf{e}_3 = \lambda_1\lambda_2\mathbf{e}_3 \qquad (5.1)$$

According to [10], the eigenvalues λ_1 and λ_2 can be considered as a $\cos^2$-decomposition of the local amplitude. Hence, these two eigenvalues can be obtained from two angular windowing functions, which are oriented along the principal axes. This means that λ_1 is obtained by convolving the signal with $\cos^2(\beta - \theta_0)$ and λ_2 is the output of convolving the signal with $\cos^2(\beta - (\theta_0 + \frac{\pi}{2})) = \sin^2(\beta - \theta_0)$. Here, θ_0 refers to the local main orientation. These two angular windowing functions are even with respect to the principal axes oriented along θ_0 and $\theta_0 + \frac{\pi}{2}$, respectively, see Fig.3.1. Thus, $\mathbf{d}_e$ has the even-even symmetry with respect to the principal axes.

The odd part of the monogenic curvature signal is computed as

$$\mathbf{d}_o = \mathbf{e}_1(T_{o11}T_{o22} - T_{o12}T_{o21}) = (\mathbf{e}_1 h_2 \mathbf{e}_3) * \mathbf{d}_e = B\mathbf{e}_1 + C\mathbf{e}_2 \qquad (5.2)$$

According to the analysis in Section 4.2, the two components of $\mathbf{d}_o$ are obtained from the second order spherical harmonic transform. Therefore, the symmetry of the odd part can be determined by the second order spherical harmonic. As visualized in Fig. 5.3, the two components of the second order spherical harmonic are odd-odd symmetric with respect to $\mathbf{e}_1$, $\mathbf{e}_2$ axes and the diagonals of the plane $\mathbf{e}_1 \wedge \mathbf{e}_2$, respectively. These
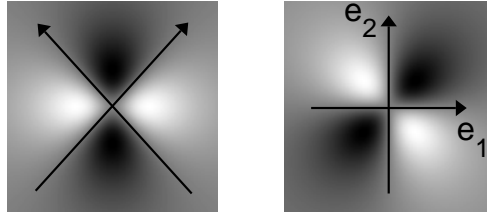
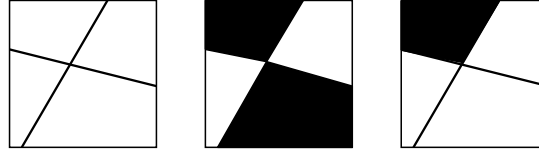Fig. 5.3: Two orthogonal components of the second order spherical harmonic.

Fig. 5.4: Some i2D Structures: from left to right are the line-like intersection, edge-like intersection and a mixture of them.

two components together decide the local main orientation. Thus, the principal axes are oriented along the local main orientation and its perpendicular orientation. Therefore, the odd part of the monogenic curvature signal, which is the vector sum of $B\mathbf{e}_1$ and $C\mathbf{e}_1$, has an odd-odd symmetry with respect to the principal axes. Hereby, we understand that the parity symmetry for i2D structures, in the presented way of analyzing the monogenic curvature tensor, is even-even and odd-odd symmetric with respect to the principal axes. At those i2D neighborhoods, even and odd outputs of the monogenic curvature signal are quite similar like the first and fourth components of the quaternionic analytic signal. But, in contrast to the quaternionic analytic signal, the parity symmetry in the current case is related to the principal axes instead of the original x, y coordinates and therefore the rotation invariance is preserved.

Unlike the i1D signals, i2D signals have more degrees of freedom. There is no general way to completely specify the parity symmetry of an arbitrary i2D structure by applying a pre-defined phase model. Because the odd part of the monogenic curvature signal has only odd-odd symmetry with respect to the principal axes, the derived phase information can only be used to classify some specific i2D structures, even though the monogenic curvature signal is a general local representation for all i2D structures. It can be assumed that a component wise evaluation of the monogenic curvature tensor will result in a more detailed specification of the parity symmetry.

For any superimposed i2D signals, as shown in Fig. 5.4, there exist patterns such as the line-like intersection, the edge-like intersection and a mixture of them. The local neighborhood where two lines/edges intersect is considered as the i2D structure. It corresponds to elliptic or hyperbolic region with positive or negative Gaussian curvature, see also table 3.1. Therefore, for the i2D neighborhood where two lines intersect, it belongs to the elliptic region which denotes local extrema. Hence, the even output of the monogenic curvature signal is positive, i.e. $\mathbf{d}_e > 0$. According to the introduction in Section 5.1, line-like structure has no odd output. Thus, for the line-like intersection structure, the odd output would vanish, i.e. $\mathbf{d}_o = 0$. In this case, the estimated local
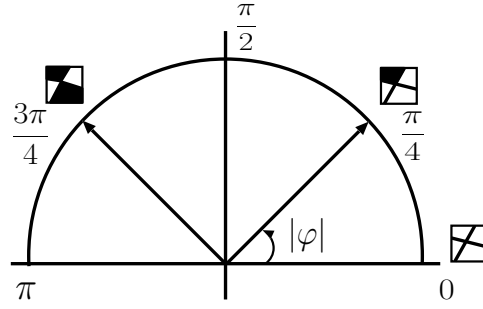
Fig. 5.5: Local phase and corresponding i2D structures. The horizontal axis is the real axis, the vertical axis indicates the imaginary axis.

phase has a value of zero

$$\varphi = \text{atan2}(\mathbf{d}_o, \mathbf{d}_e) = 0 \tag{5.3}$$

Edge-like intersection structures are saddle points which correspond to hyperbolic regions. Therefore, the monogenic curvature signal in such case has negative even outputs, i.e. $\mathbf{d}_e < 0$. It is described in Section 5.1 that edge-like structures have odd outputs. Hence, due to the intersection of edges, the monogenic curvature signal has not only even but also non-zero odd outputs. As mentioned in Section 4.2, the energy of the even part is identical to that of the odd part. Thereby, the amplitude of the even output equals that of the odd part, i.e. $|\mathbf{d}_e| = |\mathbf{d}_o|$. Hence, the absolute phase value $|\varphi|$ reads

$$|\varphi| = \text{atan2}(|\mathbf{d}_o|, \mathbf{d}_e) = \frac{3\pi}{4} \tag{5.4}$$

The sign of the phase depends on the direction of $\mathbf{d}_o$, see Eq. (4.7).

The i2D structure which is the mixture of the line-like and edge-like intersection, has also a positive even output since it corresponds to the local extrema. Due to the edge-like intersection, its odd output is also non-zero. Therefore, the even part of the monogenic curvature signal is positive, i.e. $\mathbf{d}_e > 0$. And the odd part of it is also equivalent to the even part, i.e. $|\mathbf{d}_e| = |\mathbf{d}_o|$. Thereby, for the mixture pattern, its local phase absolute value is obtained as

$$|\varphi| = \text{atan2}(|\mathbf{d}_o|, \mathbf{d}_e) = \frac{\pi}{4} \tag{5.5}$$

Its sign also relies on the direction of $\mathbf{d}_o$.

Consequently, some specific structures can be classified on the basis of the newly developed phase information. On the oriented complex plane, shown in Fig. 5.5, phase values clearly denote what kind of structure it is. The local phase is able to distinguish between line-like, edge-like intersection structures and the mixture pattern of them.

The two superimposed i1D signals are not necessarily to be perpendicular to each other. This is a meaningful extension of the structure multivector model as proposed in [10]. If the phase has a value of zero, the corresponding structure is indicating line-like intersection. A phase absolute value of $\frac{3\pi}{4}$ or $\frac{\pi}{4}$ implies that the corresponding local structure is edge-like intersection or a mixture pattern.
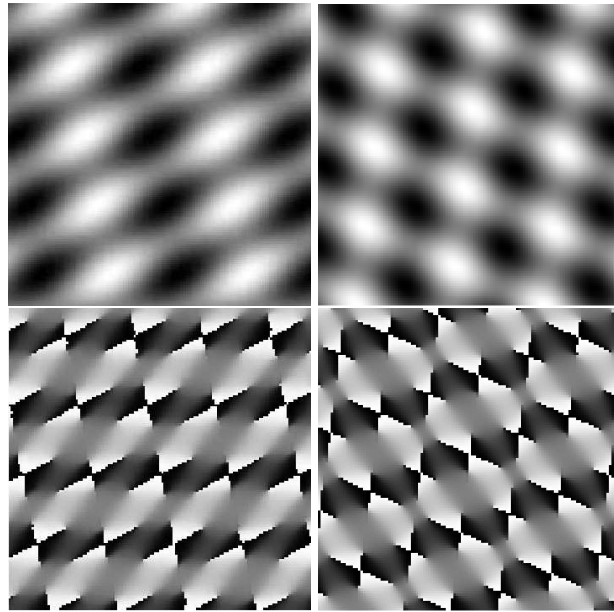
Fig. 5.6: Top row: two test images. Bottom row: corresponding phases of the two test images.

Fig. 5.6 illustrates the evaluated phase information for two superimposed patterns with flexible opening angles. In the case of very bright blobs, they can be regarded as line-like intersections, hence, their phases take zero values. For those blobs which are a bit darker than the bright blobs, they indicate edge-like intersections with phases of $\frac{3\pi}{4}$ or $-\frac{3\pi}{4}$. It can be assumed that an extensive analysis of the inner structure of the monogenic curvature tensor will yield more degrees of freedom. Thus, more phase angles will be obtained which can further help specifying i2D patterns.

6. MONOGENIC CURVATURE SCALE-SPACE

In Section 2.2, the way to embed a 2D signal into a 3D space has been introduced. So far, we discussed only the case with $z = 0$ for our general model. The half space $z > 0$ for the monogenic signal is the monogenic scale-space [15] which has already been investigated in detail. Now, we will sketch in this section the monogenic curvature signal in the half space $z > 0$. Similar as in the case of the monogenic signal, z works as a scale parameter. By applying Poisson filtering to the monogenic curvature signal results in a monogenic curvature scale-space which enables the multi-scale processing of local structures. Since the monogenic curvature signal consists of even and odd parts, the monogenic curvature scale-space can also be formed by the Poisson curvature scale-space and the conjugate curvature scale-space as illustrated in Fig. 6.1.

Combining the Poisson kernel with 2D spherical harmonics forms damped spherical harmonics which are basis functions to build the monogenic curvature scale-space. An nth order damped spherical harmonic in the frequency domain is given by

$$H_n(\rho, \alpha; s) = \exp(n\alpha \mathbf{e}_{12})\exp(-2\pi\rho s) \tag{6.1}$$

where ρ, α indicates the spectral domain polar coordinates, s denotes the scale parameter. When s equals zero, the first order damped spherical harmonic is basically identical to the Riesz kernel. Let r, β be the polar coordinates in the spatial domain, the Poisson scale-space $\mathbf{d}_e(r, \beta; s)$ can thus be obtained from the curvature tensor $T_e(r, \beta; s)$. This curvature tensor results from a scale dependent tensor valued filter which in the Fourier domain reads

$$H_e(\rho, \alpha; s) = \begin{bmatrix} H_0(\rho, \alpha; s) + \langle H_2(\rho, \alpha; s) \rangle_0 & -\langle H_2(\rho, \alpha; s) \rangle_2 \\ \langle H_2(\rho, \alpha; s) \rangle_2 & H_0(\rho, \alpha; s) - \langle H_2(\rho, \alpha; s) \rangle_0 \end{bmatrix} \tag{6.2}$$
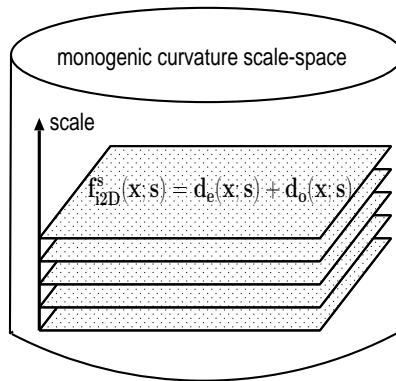

Fig. 6.1: The monogenic curvature scale-space.

By computing the Gaussian curvature of $T_e(r, \beta; s)$, the Poisson curvature scale-space is obtained as

$$
\begin{aligned}
\mathbf{d}_e(r, \beta; s) &= \det_R(T_e(r, \beta; s))\mathbf{e}_3 && (6.3) \\
&= (T_{e11}(r, \beta; s)T_{e22}(r, \beta; s) - T_{e12}(r, \beta; s)T_{e21}(r, \beta; s))\mathbf{e}_3 \\
&= A(r, \beta; s)\mathbf{e}_3
\end{aligned}
$$

The monogenic extension of the curvature tensor in the scale-space results in its conjugate part, i.e. $T_o(r, \beta; s)$. In this case, the conjugate part can be considered as the result of applying the conjugate Poisson filtering to the curvature tensor

$$
T_o(r, \beta; s) = h_1(r, \beta; s) *_\tau T_e(r, \beta; s) \tag{6.4}
$$

where $h_1(r, \beta; s)$ indicates the conjugate Poisson kernel in the spatial domain. As an alternative, $T_o(r, \beta; s)$ can also be obtained from a scale dependent tensor valued filter $H_o(\rho, \alpha; s)$, that is

$$
\begin{aligned}
T_o(r, \beta; s) &= \mathcal{F}^{-1}\left\{H_o(\rho, \alpha; s) \times_\tau \mathbf{F}(\rho, \alpha)\right\} && (6.5) \\
&= \mathcal{F}^{-1}\left\{H_1(\rho, \alpha; s) \times_\tau H_e(\rho, \alpha; s) \times_\tau \mathbf{F}(\rho, \alpha)\right\}
\end{aligned}
$$

Hence, the filter $H_o(\rho, \alpha; s)$ results from the conjugate Poisson filtering of the filter $H_e(\rho, \alpha; s)$,

$$
H_o(\rho, \alpha; s) = H_1 \times_\tau (\rho, \alpha; s)H_e(\rho, \alpha; s) = \begin{bmatrix} H_{o11}(\rho, \alpha; s) & H_{o12}(\rho, \alpha; s) \\ H_{o21}(\rho, \alpha; s) & H_{o22}(\rho, \alpha; s) \end{bmatrix} \tag{6.6}
$$

with

$$
H_{o11}(\rho, \alpha; s) = H_1(\rho, \alpha; s)(H_0(\rho, \alpha; s) + \langle H_2(\rho, \alpha; s)\rangle_0) \tag{6.7}
$$

$$
H_{o12}(\rho, \alpha; s) = -H_{o12}(\rho, \alpha; s) = H_1(\rho, \alpha; s)(-\langle H_2(\rho, \alpha; s)\rangle_2) \tag{6.8}
$$

$$
H_{o22}(\rho, \alpha; s) = H_1(\rho, \alpha; s)(H_0(\rho, \alpha; s) - \langle H_2(\rho, \alpha; s)\rangle_0) \tag{6.9}
$$

Hence, the conjugate Poisson curvature scale-space can be written as

$$
\begin{aligned}
\mathbf{d}_o(r, \beta; s) &= \mathbf{e}_1\det_R(T_o(r, \beta; s)) && (6.10) \\
&= \mathbf{e}_1(T_{o11}(r, \beta; s)T_{o22}(r, \beta; s) - T_{o12}(r, \beta; s)T_{o21}(r, \beta; s)) \\
&= B(r, \beta; s)\mathbf{e}_1 + C(r, \beta; s)\mathbf{e}_2
\end{aligned}
$$

Combining the Poisson curvature scale-space and the conjugate Poisson curvature scale-space, the monogenic curvature scale-space can be obtained, which in terms of Cartesian coordinates is given as

$$
\mathbf{f}_{i2D}^s(\mathbf{x}; s) = \mathbf{d}_e(\mathbf{x}; s) + \mathbf{d}_o(\mathbf{x}; s) \tag{6.11}
$$

According to the analysis in Section 2.1, local amplitude and local phase representation of the monogenic curvature scale-space are extracted as

$$
A(\mathbf{x}; s) = |\mathbf{f}_{i2D}^s(\mathbf{x}; s)| = \exp(\log(|\mathbf{f}_{i2D}^s(\mathbf{x}; s)|)) = \exp(\langle\log(\mathbf{e}_3\mathbf{f}_{i2D}^s(\mathbf{x}; s))\rangle_0) \tag{6.12}
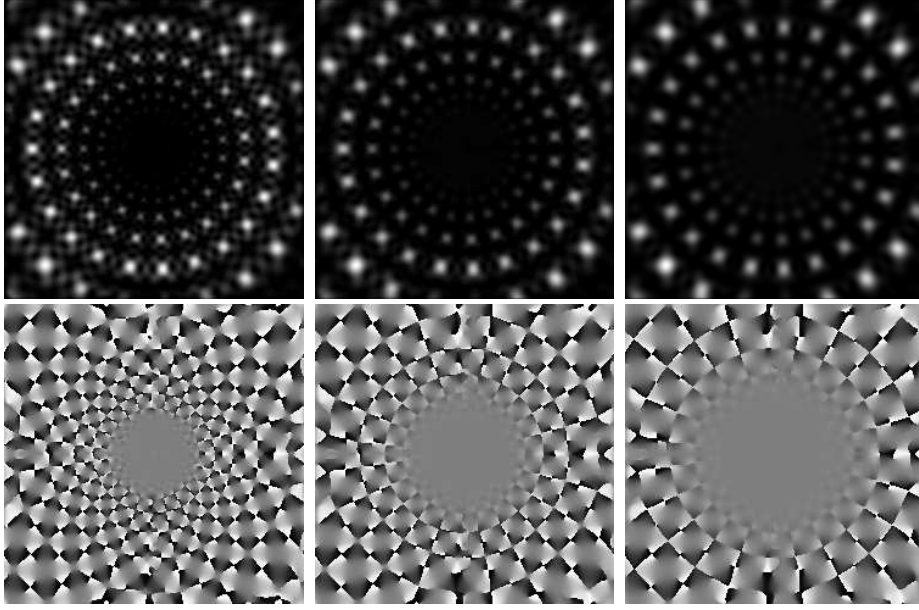$$

Fig. 6.2: Top row: local energies extracted at three scales in the monogenic curvature scale-space. Bottom row: local phases evaluated at three scales.

$$\Phi(\mathbf{x}; s) = \arg\left(\mathbf{f}_{i2D}^s(\mathbf{x}; s)\right) = \left\langle \log\left(\mathbf{e}_3 \mathbf{f}_{i2D}^s(\mathbf{x}; s)\right)\right\rangle_2 \tag{6.13}$$

As the dual of the local phase representation, the local rotation vector is defined as

$$\mathbf{r}(\mathbf{x}; s) = \arg\left(\mathbf{f}_{i2D}^s(\mathbf{x}; s)\right)^* = \left\langle \log\left(\mathbf{e}_3 \mathbf{f}_{i2D}^s(\mathbf{x}; s)\right)\right\rangle_2^* \tag{6.14}$$

The length of the rotation vector $\mathbf{r}(\mathbf{x}; s)$ indicates the angle of phase at a certain scale, and it is also perpendicular to the local orientation. Fig. 6.2 illustrates local energies and local phases extracted at three scales in the monogenic curvature scale-space. All the extracted features are scale dependent, however, local amplitude, phase and orientation are still independent of each other at each scale. Hence, the split of identity is still preserved in the monogenic curvature scale-space. For the feature extraction of the bandpassed version in the monogenic curvature scale-space, one may refer to Fig. 4.2.

Since the monogenic curvature signal is derived from the Gaussian curvature, the scale-space representation of the monogenic curvature signal is sensitive to the curvature of local structures at the chosen scale. A similar concept is the Gaussian curvature scale-space [33], which is also suitable for recovering invariant geometric features of a signal at multiple scales. However, it applies a Gaussian smoothing kernel instead of a Poisson kernel and it has a totally different curvature definition. Hence, the unique advantage of the monogenic curvature scale-space is the odd part being in quadrature phase relation to the even part at each scale. Besides, local amplitude, phase and orientation, which are unified with the scale concept, can be simultaneously estimated. These advantages give access to a multi-scale phase-based processing in many computer vision tasks.

7. CONCLUSIONS

A general signal model for 2D image structures is proposed in this paper. In order to obtain more degrees of freedoms for modeling, a 2D signal is embedded into a certain geometric algebra of the Euclidean 3D space. Coupling methods of tensor algebra, differential geometry, monogenic signal and quadrature filter, we are able to design a curvature tensor and its monogenic extension. The monogenic extension of the curvature tensor contains rich information for 2D structures as the generalization of the analytic signal to 2D case. Therefore, it is regarded as the general model for 2D image structures. Based on it, local representations for i1D and i2D structures are obtained as the monogenic signal and the monogenic curvature signal by computing the mean and Gaussian curvatures of the general model. Hence, the monogenic signal for i1D structures can be considered as a special case of the proposed general model.

From the monogenic curvature signal, three features can be extracted. They are the local amplitude, local phase and local orientation. These features are independent of each other, hence, the monogenic curvature signal performs a split of identity. The local amplitude derived from that model represents the energetic information and it indicates the existence of i2D structures. Structure information of i2D structures is contained in the local phase, and some specific types of i2D structures can be classified by the local phase. Local orientation denotes the main orientation and it illustrates the geometric information of i2D structures. Compared with other approaches for the i2D structure representation, the monogenic curvature signal has remarkable advantage of simultaneous estimation of local amplitude, local phase and local orientation in a rotation-invariant manner.

A monogenic curvature scale-space is built by applying the Poisson kernel to the monogenic curvature signal. The local amplitude, local phase and local orientation are scale dependent, but they are still independent of each other at every scale. In contrast to the Gaussian curvature scale-space, not only the energetic but also the structure and geometric information can be extracted at the same time in a multi-scale way. This advantage delivers access to various applications of the monogenic curvature signal in computer vision tasks.

APPENDIX

.1 Eigenvalues of commutative hypercomplex matrices

Commutative hypercomplex algebras (**HCA**) are the hypercomplex algebras which have similar construction rules as the Clifford algebra but with commutative multiplication rules.

In [9], Davenport proposed the four dimensional commutative hypercomplex algebras (**HCA**$_4$). It was shown that **HCA**$_4$ are isomorphic to the two-fold tensor product and the Cartesian product of the complex algebras $\mathbb{C}^2$. Later on, Felsberg et al. [11] extended the **HCA** to any 2^n dimensionas and proved that the 2^n-dimensional **HCA** are isomorphic to $\mathbb{C}^{2^{n-1}}$. The four dimensional commutative hypercomplex algebras are also isomorphic to the reduced biquaternions which are used for the signal processing [37, 36].

A four dimensional commutative hypercomplex number is defined as

$$z = z_1 + z_2 i + z_3 j + z_4 k = (z_1 + z_2 i) + (z_3 + z_4 i)j \tag{.1}$$

where i, j, k are unit basis which obey the following rules,

$$ij = ji = k,\ jk = kj = i,\ ik = ki = -j,\ i^2 = k^2 = -1,\ j^2 = 1 \tag{.2}$$

In contrast to the definition in [9], only the square of j is chosen to be positive one, which results in more simple computations.

According to the above rules, z can be reformulated as

$$
\begin{aligned}
z &= \{(z_1 + z_3) + i(z_2 + z_4)\} \left[\frac{1+j}{2}\right] + \{(z_1 - z_3) + i(z_2 - z_4)\} \left[\frac{1-j}{2}\right] \tag{.3}\\
&= \xi r_1 + \eta r_2
\end{aligned}
$$

with

$$\xi = (z_1 + z_3) + i(z_2 + z_4) \tag{.4}$$
$$\eta = (z_1 - z_3) + i(z_2 - z_4) \tag{.5}$$
$$r_1 = \frac{1+j}{2} \tag{.6}$$
$$r_2 = \frac{1-j}{2} \tag{.7}$$

Correspondingly, a four dimensional commutative hypercomplex matrix $M_{\mathbf{HCA}_4}$ can be represented as the linear composition of two complex matrices with the following form

$$M_{\mathbf{HCA}_4} = M_\xi r_1 + M_\eta r_2 \tag{.8}$$

For an $n \times n$ $M_{\mathbf{HCA}_4}$ matrix, there are n eigenvalues of each of the corresponding complex matrix. Hence, there are n^2 eigenvalues for this $M_{\mathbf{HCA}_4}$ matrix.

In the following, we restrict ourselves to the eigenvalues computation of a 2×2 matrix. Let $\lambda_{\xi 1}$, $\lambda_{\xi 2}$, $\lambda_{\eta 1}$ and $\lambda_{\eta 2}$ be the eigenvalues of complex matrices M_ξ and M_η

respectively, then the eigenvalues of the commutative hypercomplex matrix are given by

$$
\begin{aligned}
\lambda_1 &= \lambda_{\xi 1} r_1 + \lambda_{\eta 1} r_2 \\
\lambda_2 &= \lambda_{\xi 1} r_1 + \lambda_{\eta 2} r_2 \\
\lambda_3 &= \lambda_{\xi 2} r_1 + \lambda_{\eta 1} r_2 \\
\lambda_4 &= \lambda_{\xi 2} r_1 + \lambda_{\eta 2} r_2
\end{aligned}
\tag{.9}
$$

For example, given an 2×2 $M_{\mathbf{HCA}_4}$ matrix

$$
M_{\mathbf{HCA}_4} = \begin{bmatrix} 1 & i \\ j & k \end{bmatrix} = \begin{bmatrix} 1 & i \\ 0 & 0 \end{bmatrix} + \begin{bmatrix} 0 & 0 \\ 1 & i \end{bmatrix} j = \begin{bmatrix} 1 & i \\ 1 & i \end{bmatrix} r_1 + \begin{bmatrix} 1 & i \\ -1 & -i \end{bmatrix} r_2 = M_\xi r_1 + M_\eta r_2 \tag{.10}
$$

The eigenvalues of matrices M_ξ and M_η are respectively obtained as follows

$$
\lambda_{\xi 1} = 0,\ \lambda_{\xi 2} = 1 + i,\ \lambda_{\eta 1} = 0,\ \lambda_{\eta 2} = 1 - i \tag{.11}
$$

Hence, according to Eq. (.9), the four eigenvalues of the commutative hypercomplex matrix read

$$
\lambda_1 = 0 \quad \lambda_2 = \frac{1-i}{2} - \frac{1-i}{2} j \quad \lambda_3 = \frac{1+i}{2} + \frac{1+i}{2} j \quad \lambda_4 = 1 + k \tag{.12}
$$

.2   Eigenvalue computation of the Hessian matrix

According to the definition of the 4D commutative hypercomplex number, we can identify its unit basis i, j and k with the following basis elements in $\mathbb{R}_3$

$$
i \to \mathbf{e}_{12} \quad j \to \mathbf{e}_3 \quad k \to \mathbf{e}_{123} \tag{.13}
$$

The property of the unit basis based on the chosen elements can be checked as follows

$$
\begin{aligned}
i^2 = (\mathbf{e}_{12})^2 = k^2 = (\mathbf{e}_{123})^2 &= -1 \quad j^2 = (\mathbf{e}_3)^2 = 1 \\
ij = \mathbf{e}_{12}\mathbf{e}_3 = ji = \mathbf{e}_3\mathbf{e}_{12} &= \mathbf{e}_{123} = k \\
jk = \mathbf{e}_3\mathbf{e}_{123} = kj = \mathbf{e}_{123}\mathbf{e}_3 &= \mathbf{e}_{12} = i \\
ik = \mathbf{e}_{12}\mathbf{e}_{123} = ki = \mathbf{e}_{123}\mathbf{e}_{12} &= -\mathbf{e}_3 = -j
\end{aligned}
\tag{.14}
$$

Hence, the Hessian matrix in the algebraically extended framework can be considered as a commutative hypercomplex matrix, that is

$$
H_M = \begin{bmatrix} f_{xx}\mathbf{e}_3 & -f_{xy}\mathbf{e}_{123} \\ f_{xy}\mathbf{e}_{123} & f_{yy}\mathbf{e}_3 \end{bmatrix} = \begin{bmatrix} f_{xx}j & -f_{xy}k \\ f_{xy}k & f_{yy}j \end{bmatrix} \tag{.15}
$$

The above equation can further be written as

$$
\begin{bmatrix} f_{xx}j & -f_{xy}k \\ f_{xy}k & f_{yy}j \end{bmatrix} = \begin{bmatrix} 0 & 0 \\ 0 & 0 \end{bmatrix} + \begin{bmatrix} f_{xx} & -f_{xy}i \\ f_{xy}i & f_{yy} \end{bmatrix} j \tag{.16}
$$

Two corresponding complex matrices M_ξ and M_η are obtained as follows

$$M_\xi = \begin{bmatrix} f_{xx} & -f_{xy}i \\ f_{xy}i & f_{yy} \end{bmatrix} \quad M_\eta = \begin{bmatrix} -f_{xx} & f_{xy}i \\ -f_{xy}i & -f_{yy} \end{bmatrix} \tag{.17}$$

The eigenvalues of M_ξ read

$$\lambda_{\xi 1} = m \quad \lambda_{\xi 2} = n \tag{.18}$$

These two eigenvalues are equivalent to those of the real valued Hessian matrix H_R, that is

$$H = \begin{bmatrix} f_{xx} & f_{xy} \\ f_{xy} & f_{yy} \end{bmatrix} \quad \text{with} \quad \det_R(H) = mn \tag{.19}$$

Accordingly, eigenvalues of M_η are given by

$$\lambda_{\eta 1} = -n \quad \lambda_{\eta 2} = -m \tag{.20}$$

Combining eigenvalues of the two matrices M_ξ and M_η, the four eigenvalues of the algebraically extended Hessian matrix are

$$\lambda_1 = \frac{m-n}{2} + \frac{m+n}{2}j \quad \lambda_2 = \frac{m-m}{2} + \frac{m+m}{2}j = mj \tag{.21}$$

$$\lambda_3 = \frac{n-n}{2} + \frac{n+n}{2}j = nj \quad \lambda_4 = \frac{n-m}{2} + \frac{n+m}{2}j \tag{.22}$$

Hence, the determinant of the Hessian in the extended algebraic framework reads

$$\begin{aligned} \det_M(H_M) &= [(f_{xx}\mathbf{e}_3)(f_{yy}\mathbf{e}_3) - (-f_{xy}\mathbf{e}_{123})(f_{xy}\mathbf{e}_{123})]^2 = \left[f_{xx}f_{yy} - f_{xy}^2 \right]^2 \\ &= \lambda_1\lambda_2\lambda_3\lambda_4 = (mn)^2 = (\det_R(H_M))^2 \end{aligned} \tag{.23}$$

It can be concluded that the determinant computation of the Hessian in this framework can be reduced to the determinant definition as the one in the vector algebra.

The corresponding trace of the Hessian equals half of the sum of eigenvalues

$$\text{trace}_M(H_M) = f_{xx}\mathbf{e}_3 + f_{yy}\mathbf{e}_3 = \frac{1}{2}(\lambda_1 + \lambda_2 + \lambda_3 + \lambda_4) = (m+n)j = (m+n)\mathbf{e}_3 \tag{.24}$$

BIBLIOGRAPHY

[1] R. Ablamowicz. *Clifford Algebras with Numeric and Symbolic Computations*. Birkhäuser, Boston, 1996.

[2] R. Bracewell. *Fourier Analysis and Imaging*. Kluwer Academic / Plenum Publishers, New York, 2003.

[3] F. Brackx, B. De Knock, and H. De Schepper. Generalized multi-dimensional Hilbert transforms in clifford analysis. *International Journal of Mathematics and Mathematical Sciences (IJMMS)*. to appear.

[4] F. Brackx, B. De Knock, and H. De Schepper. Generalized multi-dimensional Hilbert transforms involving spherical monogenics in the framework of Clifford analysis. In *In: Extended abstracts of the ICNAAM 2005 Conference*, Rhodos, Greece, 2005.

[5] T. Bülow. Hypercomplex spectral signal representations for the processing and analysis of images. Technical Report No. 9903, Christian-Albrechts-Universität zu Kiel, Institut für Informatik und Praktische Mathematik, 1999.

[6] T. Bülow and G. Sommer. Hypercomplex signals - a novel extension of the analytic signal to the multidimensional case. *IEEE Transactions on Signal Processing*, 49(11):2844–2852, 2001.

[7] M. P. Do Carmo. *Differential geometry of curves and surfaces*. NJ: Prentice-Hall, 1976.

[8] P. E. Danielsson, Q. Lin, and Q. Z. Ye. Efficient detection of second-degree variations in 2d and 3d images. *Journal of Visual Communication and Image Representation*, 12(3):255–305, 2001.

[9] C. M. Davenport. A commutative hypercomplex algebra with associated function theory. pages 213–227, 1996.

[10] M. Felsberg. Low-level image processing with the structure multivector. Technical Report No. 2016, Christian-Albrechts-Universität zu Kiel, Institut für Informatik und Praktische Mathematik, 2002.

[11] M. Felsberg, T. Bülow, and G. Sommer. Commutative hypercomplex Fourier transforms of multidimensional signals. In G. Sommer, editor, *Geometric Computing with Clifford Algebra*, pages 209–229. Springer-Verlag, Heidelberg, 2001.

[12] M. Felsberg and E. Jonsson. Energy tensors: Quadratic phase invariant image operators. In *Pattern Recognition 2005*, volume 3663 of *LNCS*, pages 493–500. Springer, 2005.

[13] M. Felsberg and U. Köthe. Get: The connection between monogenic scale-space and gaussian derivatives. In R. Kimmel, N. Sochen, and J. Weickert, editors, *Scale Space and PDE Methods in Computer Vision*, volume 3459 of *LNCS*, pages 192–203. Springer, 2005.

[14] M. Felsberg and G. Sommer. The monogenic signal. *IEEE Transactions on Signal Processing*, 49(12):3136–3144, December 2001.

[15] M. Felsberg and G. Sommer. The monogenic scale-space: A unifying approach to phase-based image processing in scale-space. *Journal of Mathematical Imaging and Vision*, 21:5–26, 2004.

[16] L. Florack. *Image Structure*, volume 10 of *Computational Imaging and Vision*. Kluwer Academic Publishers, 1997.

[17] L. M. J. Florack, B. M. ter Haar Romeny, J. J. Koenderink, and M. A. Viergever. Cartesian differential invariants in scale-space. *Math. Imaging Vision*, 3(4):327–348, 1993.

[18] W. Förstner and E. Gülch. A fast operator for detection and precise location of distinct points, corners and centers of circular features. In *Proc. ISPRS Intercommission Conference on Fast Processing of Photogrammetric Data*, pages 281–305, Interlaken, Switzerland, June 1987.

[19] W. T. Freeman and E. H. Adelson. The design and use of steerable filters. *IEEE Trans. Pattern Analysis and Machine Intelligence*, 13(9):891–906, 1991.

[20] D. Gabor. Theory of communication. *Journal of the IEE*, 93:429–457, 1946.

[21] G. H. Granlund and H. Knutsson. *Signal Processing for Computer Vision*. Kluwer Academic Publishers, Dordrecht, 1995.

[22] S.L. Hahn. *Hilbert Transforms in Signal Processing*. Artech House, Boston, London, 1996.

[23] D. Hestenes, H. Li, and A. Rockwood. Geometric computing with Clifford algebras. In G. Sommer, editor, *New Algebraic Tools for Classical Geometry*, pages 3–23. Springer-Verlag, 2001.

[24] D. Hestenes and G. Sobczyk. *Clifford Algebra to Geometric Calculus*. Reidel, Dordrecht, 1984.

[25] J. J. Koenderink and A. J. van Doorn. Representation of local geometry in the visual system. *Biological Cybernetics*, 55:367–375, 1987.

[26] J. J. Koenderink and A. J. van Doorn. Two-plus-one-dimensional differential geometry. *Pattern Recogn. Lett.*, 15(5):439–443, 1994.

[27] U. Köthe. Integrated edge and junction detection with the boundary tensor. In *Proceeding of 9th Intl. Conf. on Computer Vision*, volume 1, pages 424–431, 2003.

[28] M. Krause and G. Sommer. A 3d isotropic quadrature filter for motion estimation problems. In *Proc. Visual Communications and Image Processing, Beijing, China*, volume 5960, pages 1295–1306. The International Society for Optical Engineering, Bellingham, 2005.

[29] G. Krieger and C. Zetzsche. Nonlinear image operators for the evaluation of local intrinsic dimensionality. *IEEE Transactions on Image Processing*, 5(6):1026–1042, June 1996.

[30] N. Krüger and M. Felsberg. A continuous formulation of intrinsic dimension. In *British Machine Vision Conference*, 2003.

[31] P. Lounesto. *Clifford Algebras and Spinors*. Cambridge University Press, 1997.

[32] F. Mokhtarian and M. Bober. *Curvature scale space representation: theory, applications, and MPEG-7 standardization*. Kluwer Academic Publishers, 2003.

[33] F. Mokhtarian and R. Suomela. Robust image corner detection through curvature scale space. *IEEE Trans. on Pattern Analysis and Machine Intelligence*, 20(12):1376–1381, 12 1998.

[34] A. V. Oppenheim and J. S. Lim. The importance of phase in signals. *IEEE Proceedings*, 69:529–541, May 1981.

[35] A. Papaulis. *The Fourier Integral and its Application*. McGraw-Hill, New York, 1962.

[36] S. C. Pei, J. H. Chang, and J. J. Ding. Commutative reduced biquaternions and their Fourier transform for signal and image processing applications. *IEEE Trans. on signal processing*, 52(7):2012–2031, 2004.

[37] H. D Schütte and J. Wenzel. Hypercomplex numbers in digital signal processing. In *Proc. IEEE Int. Symp. Circuits Syst.*, volume 2, pages 1557–1560, 1990.

[38] G. Sobczyk and G. Erlebacher. Hybrid matrix geometric algebra. In H. Li, P. J. Olver, and G. Sommer, editors, *Computer Algebra and Geometric Algebra with Applications*, volume 3519 of *LNCS*, pages 191–206. Springer-Verlag, Berlin Heidelberg, 2005.

[39] G. Sommer and D. Zang. Parity symmetry in multi-dimensional signals. In *Proc. of the 4th International Conference on Wavelet Analysis and Its Applications*, Macao, 2005.

[40] C. Zetzsche and E. Barth. Fundamental limits of linear filters in the visual processing of two-dimensional signals. *Vision Research*, 30:1111–1117, 1990.

[41] C. Zetzsche and E. Barth. Image surface predicates and the neural encoding of two-dimensional signal variation. In B. Rogowitz, editor, *Proc. SPIE Human Vision and Electronic Imaging: Models, Methods and Applications*, volume 1249, pages 160–177, 1990.